Short Article

Cell Stem Cell

Adult Neural Stem Cells from the Subventricular Zone Give Rise to Reactive Astrocytes in the Cortex after Stroke

Graphical Abstract

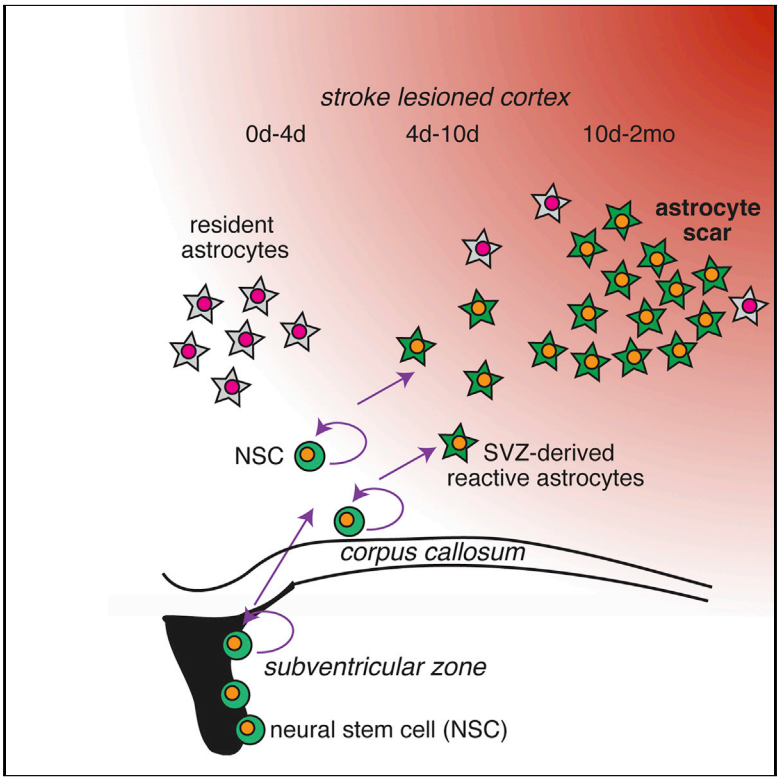

Highlights

- NS-forming NSCs found in the stroke-injured cortex originate in the SVZ
- SVZ derived cells differentiate into RAs and contribute to astrocyte scar formation
- A small population of SVZ derived NSCs persists transiently in the cortex
- Transcription factor *Ascl1* can convert SVZ derived RAs to neurons in vivo

Authors

Maryam Faiz, Nadia Sachewsky, Sergio Gascón, K.W. Annie Bang, Cindi M. Morshead, Andras Nagy

Correspondence

cindi.morshead@utoronto.ca (C.M.M.), nagy@lunenfeld.ca (A.N.)

In Brief

Faiz and colleagues show that self-renewing, multipotent neural stem cells in the subventricular zone leave their niche and migrate to the site of injury following stroke. These migratory stem cells give rise to reactive astrocytes that contribute to astrocyte scar formation.

Faiz et al., 2015, Cell Stem Cell *17*, 624–634
November 5, 2015 ©2015 Elsevier Inc.
http://dx.doi.org/10.1016/j.stem.2015.08.002

CellPress

Cell Stem Cell
Short Article

Adult Neural Stem Cells from the Subventricular Zone Give Rise to Reactive Astrocytes in the Cortex after Stroke

Maryam Faiz,[1] Nadia Sachewsky,[2,5] Sergio Gascón,[3,4] K.W. Annie Bang,[1] Cindi M. Morshead,[2,5,*] and Andras Nagy[1,6,*]
[1]Lunenfeld-Tanenbaum Research Institute, Mount Sinai Hospital, Toronto, ON M5T 3H7, Canada
[2]Donnelly Centre for Cellular and Biomolecular Research, University of Toronto, Toronto, ON M5S 3E1, Canada
[3]Department of Physiological Genomics, Institute of Physiology, Ludwig-Maximilians University Munich, Pettenkoferstrasse 12, Munich D-80336, Germany
[4]Institute for Stem Cell Research, Helmholtz Center Munich, Ingolstädter Landstrasse 1, Neuherberg/Munich D-85764, Germany
[5]Department of Surgery, University of Toronto, Toronto, ON M5T 1P5, Canada
[6]Department of Obstetrics and Gynecology, University of Toronto, Toronto, ON M5G 1E2, Canada
*Correspondence: cindi.morshead@utoronto.ca (C.M.M.), nagy@lunenfeld.ca (A.N.)
http://dx.doi.org/10.1016/j.stem.2015.08.002

SUMMARY

Reactive astrocytes (RAs) have been reported to convert to multipotent neural stem cells (NSCs) capable of neurosphere (NS) formation and multilineage differentiation in vitro. Using genetic tagging, we determined that subventricular zone (SVZ) NSCs give rise to NSs derived from the stroke-injured cortex. We demonstrate that these cells can be isolated from the cortex in two different models of stroke and from different stroke-lesioned cortical regions. Interestingly, SVZ NSCs give rise to a subpopulation of RAs in the cortex that contribute to astrogliosis and scar formation. Last, we show that these SVZ derived RAs can be converted to neurons in vivo by forced expression of *Ascl1*. Identifying the contribution of cells originating from the SVZ to injury repair has implications for neural regeneration strategies.

INTRODUCTION

The adult mammalian brain contains a population of neural stem cells (NSCs) in the subventricular zone (SVZ) that express NESTIN and glial fibrillary acidic protein (GFAP). Adult NSCs give rise to neuroblasts, which migrate to the olfactory bulb and generate new neurons (Lois and Alvarez-Buylla, 1994). Following brain injury, these neuroblasts can migrate to the lesion site (Arvidsson et al., 2002) following cues released by cells at the injury including reactive glia (Leong and Turnley, 2011). Nevertheless, the brain remains limited in its ability to generate new neurons after injury.

Reactive astrocytes (RAs) are a heterogeneous population of cells (Molofsky et al., 2012) that play key roles in the CNS response to injury, such as restricting inflammation, preventing neuronal loss, and repairing the blood brain barrier (Burda and Sofroniew, 2014). Recently, two types of RAs have been defined based on their structural properties: (1) newly proliferated elongated astrocytes that express progenitor markers such as SOX2, brain lipid binding protein (BLBP), and RC2, and (2) stellate astrocytes that derive from resident cortical astrocytes (Wanner et al., 2013). It has also been suggested that a subset of RAs has the potential to convert to multipotent, self-renewing NSCs capable of NS formation in vitro (Buffo et al., 2008; Shimada et al., 2012). However, a recent study has described a subpopulation of RAs originating from the SVZ that migrate to the damaged tissue and are distinct from resident RAs in a postnatal mouse model of hypoxia/ischemia (Benner et al., 2013). This led us to investigate with genetic tools: (1) the origin of cortical neurospheres in two models of stroke, and (2) the contribution of SVZ cells to the astrogliosis that is seen following brain injury.

Lineage tracking using tamoxifen inducible Nestin-CreER^{T2} (Imayoshi et al., 2006; Lagace et al., 2007) and Cre conditional reporter (Madisen et al., 2010; Srinivas et al., 2001) transgenic mice revealed that cortical NSs originate from SVZ-derived NSCs that migrate to the stroke lesion after injury. These cortical SVZ-derived cells rapidly differentiate and give rise to a subpopulation of RAs that contribute to the astrocyte scar, thus highlighting a role for the SVZ in post injury gliosis. Last, we demonstrate that the transcription factor *Ascl1* (also known as *Mash1*) can convert SVZ derived RAs to neurons, providing a new target for cellular conversion strategies aimed at enhancing neurogenesis.

RESULTS

Neurosphere Forming Capacity of Cells in the Injured Cortex

To detect NSCs in the injured adult cortex, we performed the NS assay on tissue derived from the injured cortex and the SVZ (Figure 1A) of mice 4 days after an endothelin-1 (ET-1) induced stroke. Similar to previous reports (Buffo et al., 2008; Erlandsson et al., 2011; Shimada et al., 2012), NSs formed from the SVZ and stroke-injured cortex (Figures 1B and 1C), but never from the contralateral (uninjured) cortex (Figure 1C). While the average size of cortex-derived NSs (ctxNSs) was less than SVZ derived NSs (svzNSs) (Figure S1A), both populations displayed the cardinal properties of stem cells; self-renewal and multipotency (Potten and Loeffler, 1990). Single NS passaging revealed extended self-renewal (up to passage 5, the longest time examined) with no difference in NS number at each passage (Figure S1B). Furthermore, ctxNSs and svzNSs

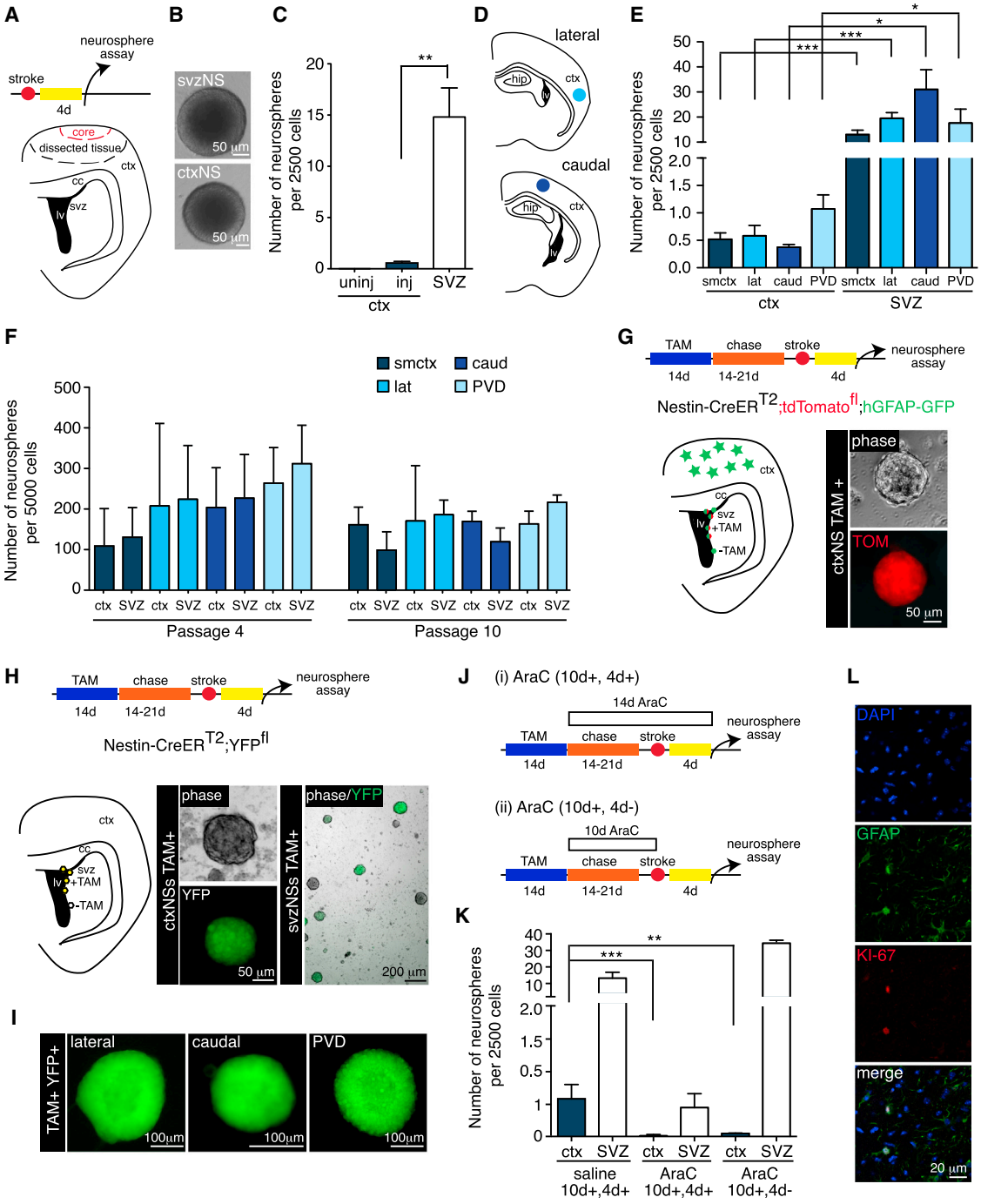

Figure 1. Migratory SVZ Cells Give Rise to Neurospheres in the Stroke-Injured Cortex

(A) Experimental design for cortical NS culture.

(B) SVZ derived and cortical derived NSs (svz and ctx).

(C) Number of NSs formed from the uninjured and stroke-injured cortex and SVZ (** = $p = 0.001$, unpaired t test with Welch's correction, $t(8) = 5.006$, data represent ±SEM, $n_{ctx} = 11$ mice, and $n_{svz} = 9$ mice).

(D) Diagram of injection sites lateral and caudal to the original sensory-motor cortex lesion site.

(E) Number of NSs formed from the cortex and SVZ in lesions lateral and caudal to the original sensory-motor cortex lesion (smctx) and after PVD (*** = $p < 0.001$, unpaired t test, $t(12) = 9.785$, data represent ±SEM, $n_{smctx\_ctx} = 9$ mice, $n_{smctx\_SVZ} = 5$ mice; *** = $p < 0.001$, unpaired t test, $t(6) = 8.454$, data represent ±SEM, $n_{lat\_ctx} = 4$ mice, $n_{lat\_SVZ} = 4$ mice; * = $p < 0.05$, unpaired t test, $t(4) = 3.908$, data represent ±SEM, $n_{caud\_ctx} = 3$ mice, $n_{caud\_SVZ} = 3$ mice; and * = $p < 0.05$, unpaired t test, $t(12) = 2.978$, data represent ±SEM, $n_{PVD\_ctx} = 7$ mice, $n_{PVD\_SVZ} = 7$ mice).

(F) Number of NSs at passage 4 and passage 10 from the original sensory-motor cortex lesion, lateral, and caudal to that site and after PVD (n.s., unpaired t test, $t(5)_{passage4\_et\text{-}1} = 0.1879$, $t(11)_{passage10\_et\text{-}1} = 1.1016$, $t(12)_{passage4\_PVD} = 0.3755$, $t(10)_{passage10\_PVD} = 1.910$, $t(3)_{passage4\_lat} = 0.07205$, $t(2)_{passage10\_late} = 0.112$,

(legend continued on next page)

were multipotent (Figure S1C), with similar differentiation profiles (Figure S1D). We asked if these findings were specific to the site of cortical injury or the model of stroke. In a first series of experiments, we assessed NS formation in response to ET-1 strokes in different regions of the cortex. NSs formed from the stroke-injured cortex at lesion sites both lateral (Figures 1D and 1E) and caudal (Figures 1D and 1E) to the sensory-motor cortex lesions originally examined, revealing that the response was not regionally specific within the cortex. In a second series of experiments, we used a different model of stroke, pial vessel disruption (PVD) (Hua and Walz, 2006; Kolb et al., 2007). PVD to the sensory-motor cortex resulted in the generation of cortical derived NSs, identical to what was observed with ET-1 stroke (Figure 1E). Bulk passaging showed that, akin to our original stroke paradigm, NSs from lateral, caudal, and PVD stroke sites showed extended passaging (up to Passage 10, the longest time examined), with no difference in NS number between ctxNSs and svzNSs (Figure 1F). Further, no difference was seen in the percent of multipotent ctxNSs versus svzNSs (Figure S1E).

Cortical Derived Neurospheres Are Derived from Migratory SVZ Stem Cells

With the goal of distinguishing between ctxNSs and svzNSs, we took advantage of the Nestin-CreER^{T2};tdTomato^{fl} double transgenic mouse (Imayoshi et al., 2006; Lagace et al., 2007), which enables permanent tdTOMATO labeling of cells expressing NESTIN during the time of Cre recombinase induction with tamoxifen. NESTIN is expressed by neural stem and progenitor cells in vivo (Morshead et al., 1994). We crossed these animals with hGFAP-GFP mice that permit visualization of GFAP expressing astrocytes and NSCs (Zhuo et al., 1997). The Nestin-CreER^{T2};tdTomato^{fl};hGFAP-GFP triple transgenic mice were fed tamoxifen for 2 weeks and chased for 2–3 weeks (Figure 1G), ensuring labeling of SVZ cells with tdTOMATO and eliminating the possibility of tamoxifen uptake by RAs that express NESTIN after stroke (Clarke et al., 1994). Tamoxifen fed triple transgenic mice gave rise to GFP+/tdTOMATO+ svzNSs, while the unfed mice gave rise to GFP+/tdTOMATO− svzNSs (Figure S1F). Most striking, all of the ctxNSs from stroke lesioned, tamoxifen fed Nestin-CreER^{T2};tdTomato^{fl};hGFAP-GFP mice were GFP+/tdTOMATO+ (Figure 1G) compared to the control unfed mice, where none of the ctxNSs expressed tdTOMATO. Based on the total number of cells we isolated from the stroke-lesioned site, we estimate that approximately 35 ctxNS forming cells are found in the injured cortex at 4 days post stroke. We repeated this experiment in a second strain of Nestin-CreER^{T2} mice (Lagace et al., 2007) to ensure that the findings were not the result of tamoxifen independent tdTOMATO expression (Imayoshi et al., 2006) or recombination in NESTIN negative cells (Sun et al., 2014). Nestin-CreER^{T2} mice were crossed with a YFP^{fl} Cre conditional reporter and fed tamoxifen for 2 weeks, followed by a 2–3 week chase (Figure 1H) to label SVZ cells and not RAs with YFP (Figure S1G). Tamoxifen fed mice gave rise to both YFP+ SVZ (Figure 1H) and ctx derived NSs (Figures 1H and S1H). Moreover, YFP+ ctxNSs were seen after ET-1 strokes both lateral and caudal to the original site, as well as after PVD lesions (Figure 1I). Importantly, the frequency of labeling in ctxNSs was similar to the frequency of labeling in the corresponding SVZ (Table S1), supporting the conclusion that ctxNSs are derived from the SVZ.

To confirm the finding that GFAP+ NSCs were giving rise to ctxNSs, we took advantage of the GFAP-TK mice (Bush et al., 1998, 1999) that express herpes simplex virus thymidine kinase (TK) from the GFAP promoter. In these mice, proliferating GFAP+ cells will undergo cell death in the presence of ganciclovir (GCV) (Imura et al., 2003; Morshead et al., 2003). Control (non-TK) mice that received an ET-1 stroke gave rise to ctxNSs in the presence of GCV, however, there was a complete loss of ctxNSs from ET-1 stroke-injured GFAP-TK mice in the presence of GCV (Figure S1I). These findings are consistent with the conclusion that ctxNSs are derived from GFAP+ NSCs.

To further demonstrate the SVZ origin of ctxNSs, we used a well-established SVZ ablation paradigm (Doetsch et al., 1999) to eliminate proliferating precursors in the SVZ. We predicted that ablating SVZ precursors would result in a loss of ctxNSs at 4 days post ET-1 stroke. Cytosine β-D-arabinoside (AraC) was intraventricularly infused prior to performing the NS assays. Nestin-CreER^{T2};tdTomato^{fl};hGFAP-GFP mice received AraC for 10 days prior to stroke and for 4 days post stroke (AraC, 10 days+ and 4 days+; Figure 1J (i)). As previously reported (Doetsch et al., 1999), AraC infusion caused a reduction in the number of svzNSs and, as predicted, virtually eliminated ctxNS formation (Figure 1K). We used KI-67 to assess the possibility that intraventricular AraC administration was depleting the proliferating cells in the stroke-injured cortex and this was accounting for the loss of NS forming cells from the cortex. Importantly, we observed KI-67+/GFAP+ cells within the injured cortex demonstrating that the intraventricular AraC infusion did not eliminate resident cortical cells that divide post stroke (Figure 1L). Hence, the loss of ctxNSs was not due to the AraC kill of mitotically active cells within the lesioned cortex, but rather was the result of eliminating proliferating SVZ cells.

Previous studies have shown the rapid repopulation of the SVZ following ablation of the neural precursor pool (Doetsch et al., 1999; Morshead et al., 1994). We reasoned that AraC withdrawal at the time of stroke would permit repopulation of the SVZ and subsequent migration of NSCs to the injured cortex.

t(4) $_{passage4\_caud}$ = 1.349, t(4) $_{passage10\_caud}$ = 0.9843, data represent ±SEM, $n_{P4\_et1\_ctx}$ = 3, $n_{P10\_et1\_ctx}$ = 6, $n_{P4\_PVD\_ctx}$ = 7, $n_{P10\_PVD\_ctx}$ = 7, $n_{P4\_lat\_ctx}$ = 2, $n_{P10\_lat\_ctx}$ = 2, $n_{P4\_caud\_ctx}$ = 2, $n_{P10\_caud\_ctx}$ = 2, $n_{P4\_et1\_SVZ}$ = 4, $n_{P10\_et1\_SVZ}$ = 7, $n_{P4\_PVD\_SVZ}$ = 6, $n_{P10\_PVD\_SVZ}$ = 6, $n_{P4\_lat\_SVZ}$ = 3, $n_{P10\_lat\_SVZ}$ = 2, $n_{P4\_caud\_SVZ}$ = 4, and $n_{P10\_caud\_SVZ}$ = 4, 3 independent trials).

(G) Lineage tracing of SVZ cells using Nestin-CreER^{T2};tdTomato^{fl};hGFAP-GFP mice. The picture shows tdTOMATO expression in ctxNSs.

(H) Lineage tracing of SVZ cells using Nestin-CreER^{T2};YFP^{fl} mice. The pictures show YFP expression in ctxNSs and SVZNSs.

(I) YFP expression in ctxNSs from stroke sites lateral and caudal to the original sensory-motor cortex lesion site and PVD.

(J) AraC ablation paradigms.

(K) Number of ctxNSs and svzNSs after AraC ablation (** = $p < 0.01$, *** = $p < 0.001$, one-way ANOVA with Tukey's post hoc, $F(2,11) = 16.91$, data represent ±SEM from (days, d) n_{saline} = 8, $n_{14dAraC}$ = 4, and $n_{10dAraC}$ = 2.

(L) KI-67 positive cells in the cortex (uninjured = uninj, injured = inj, subventricular zone = SVZ, lateral ventricle = lv, cortex = ctx, corpus callosum = cc, sensory-motor cortex = smctx, PVD, lateral = lat, caudal = caud, tdTOMATO = TOM, and tamoxifen = TAM). See also Figure S1 and Table S1.

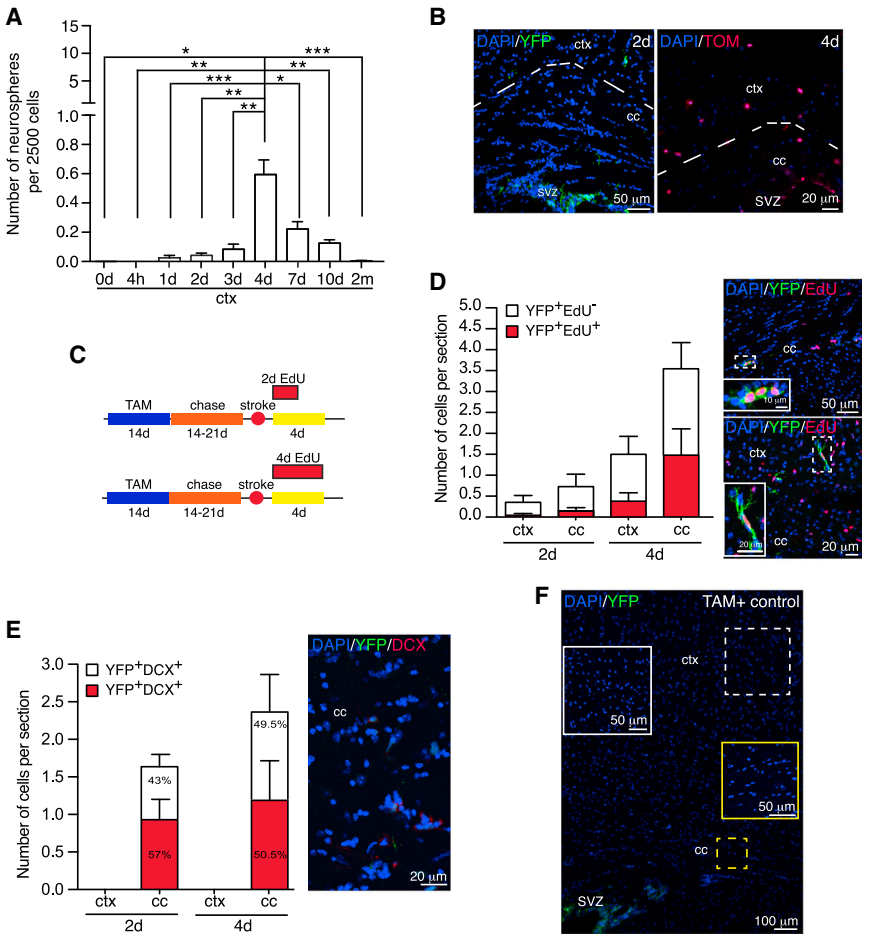

Figure 2. Characterization of Migratory SVZ Cells

(A) Number of ctxNSs (* = $p < 0.05$, ** = $p < 0.01$, *** = $p < 0.001$, one-way ANOVA with Tukey's post hoc, $F(9,70)_{ctx} = 7.669$, $F(9,61)_{svz} = 1.032$, data represent ±SEM (days, d), $n_{0dcx} = 3$, $n_{4h\_cx} = 4$, $n_{1d\_cx} = 7$, $n_{2d\_cx} = 6$, $n_{3dcx} = 7$, $n_{4d\_cx} = 21$, $n_{7d\_cx} = 7$, $n_{10d\_cx} = 8$, and $n_{2mo\_cx} = 8$).

(B) SVZ derived cells migrating to the stroke-injured cortex in Nestin-CreER^{T2};YFP^{fl} and Nestin-CreER^{T2};tdTomato^{fl};hGFAP-GFP mice.

(C) EdU labeling paradigm in Nestin-CreER^{T2};YFP^{fl} mice.

(D) YFP+EdU+ and YFP+EdU− cells in the cortex and corpus at 2 days and 4 days after stroke. The inset shows higher magnification of the boxed cell (n.s. = $p_{ctx\_2d\_vs\_4d} = 0.6644$, unpaired t test, $t(8) = 0.4504$, data represent ±SEM, $n_{2d\_ctx} = 5$ mice, and $n_{4d\_ctx} = 6$ mice and n.s. = $p_{cc\_2d\_vs\_4d} = 0.0883$, unpaired t test with Welch's correction, $t(5) = 2.113$, data represent ±SEM, $n_{2d\_cc} = 4$ mice, and $n_{4d\_cc} = 6$ mice.

(E) YFP+DCX+ and YFP+DCX− cells in the cortex and corpus callosum at 2 days and 4 days after stroke.

(F) YFP expression in TAM fed, uninjured controls. The white and yellow insets show higher magnification photos of regions in dashed white and yellow boxes (cortex = ctx, corpus callosum = cc, subventricular zone = SVZ, tdTOMATO = TOM, and tamoxifen = TAM).

To test this, AraC was infused for 10 days prior to stroke in the triple transgenic mice and the NS assay was performed 4 days later (AraC, 10 days+ and 4 days−; Figure 1J (ii)). We observed the return of svzNSs as predicted, but no concomitant increase in the number of ctxNSs on day 4 (Figure 1K). Since the lack of ctxNS formation could be due to a delay in the migration of SVZ cells to the lesion site following AraC ablation and repopulation, we compared the number of ctxNSs at 7 days post stroke in AraC treated and untreated (stroke only) wild-type mice. Interestingly, we found no difference in the numbers of ctxNSs between these groups (Figure S1J). Notably, when we compared the number of ctxNSs at 4 and 7 days in AraC untreated stroke-injured mice, the number of ctxNSs at 7 days was significantly less than what was observed at 4 days (Figure 2A). These findings suggest that repopulation of the SVZ occurs at the expense of migrating SVZ cells to the cortex. This may be the result of the cortical microenvironment being less attractive to migrating SVZ precursors at 7 days and/or the microenvironment prompting their differentiation at the site of injury.

SVZ Stem Cells Migrate to the Stroke Site and Give Rise to RAs

Next, we examined the time course of migration of SVZ cells to the site of injury. We assayed for ctxNS formation following ET-1 stroke starting at 4 hr post stroke and continuing to 2 months post stroke. As seen in Figure 2A, we observed a gradual increase in the numbers of ctxNS from 1 to 4 days. After 4 days, there was a decrease in the numbers of ctxNSs until 10 days and by 2 months virtually no ctxNSs were detected (one sphere was formed from the cortex in one of eight animals; Figure 2A). Consistent with the migration of SVZ cells to the site of injury, we observed YFP and tdTOMATO labeled cells (Figure 2B) at 2 and 4 days post stroke in the brain parenchyma of the stroke-injured mice. We characterized the SVZ derived parenchymal cells to determine the proliferation dynamics and phenotype of migratory YFP+ cells. EdU injections were given to NestinCreER^{T2};YFP^{fl} mice for 2 or 4 days after stroke (Figure 2C), and the numbers and locations of YFP+/EdU− and YFP+EdU+ cells were assessed. YFP+ cells were seen in both the corpus callosum and the cortex with no difference in the relative percentage of YFP+EdU+ cells at 2 and 4 days post stroke (Figure 2D). Further, we looked for doublecortin (DCX) expressing neuroblasts (YFP+/DCX+) en route to, and/or within, the injury site at 2 and 4 days post stroke and observed a small number of DCX+ cells in the corpus callosum (Figure 2E) at all times examined. However, no DCX+ cells were seen in the cortex at 2 days or 4 days post stroke even at a time of peak ctxNS formation (Figure 2E). YFP+ cells were never observed in the parenchyma of control (non-stroked) mice (Figure 2F). To determine if CSPG4+ cells contribute to cortical NS formation, we performed the NS assay in Cspg4-DsRed mice 4 days after stroke. We never observed DSRED+ ctxNSs (0/6 mice). These

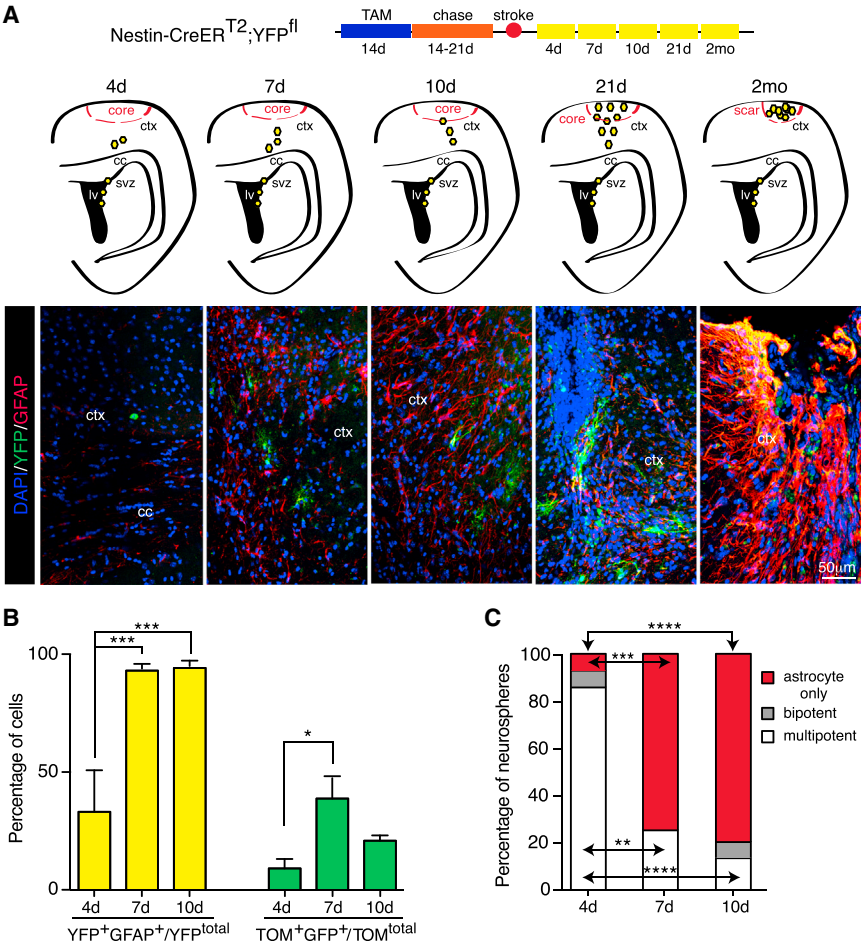

Figure 3. Migratory SVZ Cells Give Rise to Reactive Astrocytes at the Lesion Site

(A) Lineage tracing of SVZ cells using Nestin-CreER^{T2};YFP^{fl} mice. The YFP+ cells in the parenchyma are from 4 days to 2 months after stroke.

(B) Ratio of SVZ derived RAs (YFP+GFAP+/YFP^{total} or TOM+GFP+/TOM^{total}) in Nestin-CreER^{T2};YFP^{fl} and Nestin-CreER^{T2};tdTomato^{fl};hGFAP-GFP mice (* = $p < 0.05$, *** = $p < 0.001$, one-way ANOVA with Tukey's post hoc, $F(3,19)_{YFP+GFAP+/YFP^{total}} = 19.87$, data represent ±SEM, $n_{4d} = 6$ mice, $n_{7d} = 7$ mice, $n_{10d} = 7$ mice and one-way ANOVA with Tukey's post hoc, $F(3,10)_{Tom+GFP+/Tom^{total}} = 5.5852$ data represent ±SEM, $n_{4d} = 3$ mice, $n_{7d} = 4$ mice, and $n_{10d} = 4$ mice).

(C) Percentage of multipotent, bipotent, and astrocyte only ctxNSs (** = $p < 0.01$, *** = $p < 0.001$, and **** = $p < 0.0001$) (days, d) (z-test for independent proportions, $z_{4dvs7dmultipotent} = 3.123$ $z_{4dvs10dmultipotent} = 3.9155$, $z_{7dvs10dmultipotent} = 0.8007$, $z_{4dvs7dastrocyte\_only} = 3.5543$ $z_{4dvs10dastrocyte\_only} = 3.9506$, $z_{7dvs10dastrocyte\_only} = -0.3105$, data represent $n_{4d} = 14$ NSs, $n_{7d} = 12$ NSs, and $n_{10d} = 15$ NSs) (tdTOMATO = TOM, subventricular zone = SVZ, lateral ventricle = lv, cortex = ctx, corpus callosum = cc, and tamoxifen = TAM). See also Figure S2.

findings indicate that neither CSPG4+ cells nor migrating YFP+ DCX+ cells give rise to ctxNSs.

Irrespective of ctxNS formation, we consistently observed SVZ derived YFP+ cells in the cortex of stroke-injured NestinCreER^{T2};YFP^{fl} mice from 2 days to 2 months post stroke (Figures 2B and 3A). We assessed whether the SVZ derived cells were contributing to injury-induced astrogliosis. The numbers of GFAP+ astrocytes among SVZ derived cells from the cortex of Nestin-CreER^{T2};YFP^{fl} mice was assayed at 4, 7, and 10 days post stroke. Indeed, we observed a significant increase in the percentage of SVZ derived RAs (YFP+GFAP+) among total SVZ derived cells (YFP+) from 4 to 7 days and this increase was maintained at 10 days post stroke (Figure 3B). At 2 months, SVZ derived RAs were seen in the astroglial scar (Figure 3A). To further confirm our findings, we used the NestinCreER^{T2};tdTomato^{fl};hGFAP-GFP mice. Quantification of SVZ derived cells in the cortex at 4, 7, and 10 days after stroke (Figure S2A) showed a decrease in the percentage of GFP− cells among total tdTOMATO+ cells (Figure S2B) and an increase in the percentage of GFP+ cells among total tdTOMATO+ cells from 4 days to 7 days (Figure 3B). tdTOMATO+GFP+ cells were positive for S100β, further confirming astrocyte identity (Figure S2C). Given that tamoxifen fed control mice also had tdTOMATO signal in some of the vasculature in the brain (Figure S2D), we may be underestimating the contribution of SVZ derived tdTOMATO+ cells to reactive astrogliosis. Together, these findings show that SVZ derived cells migrate to the injury site and differentiate into a population of RAs.

We took advantage of the NS assay to examine the differentiation potential of ctxNS to test the prediction that ctxNS would have a higher propensity to generate astrocyte only clones when isolated at later times post stroke. Indeed, we found that ctxNSs displayed reduced multipotency when isolated at 7 and 10 days post stroke (88% multipotent NSs at 4 days and 13.3% at 10 days post stroke; Figure 3C). There was a concomitant increase in the number of ctxNSs producing astrocyte only colonies at later times post stroke (7% at 4 days and 80% at 10 days) (Figure 3C), Together, these findings support the hypothesis that SVZ derived cells migrate to the injury site post stroke and give rise to RAs.

SVZ Derived RAs Can Be Converted into Neurons

We next asked if the SVZ derived RAs could be converted to neurons. Cultures of RAs were established (S.G., unpublished data) from the stroke lesioned cortex of tamoxifen treated Nestin-CreER^{T2};YFP^{fl} double transgenic mice (Figure 4A). Within the cultures, the GFAP+ and S100β+ astrocytes were invariably YFP+, revealing that their origin was from the SVZ and resident cortical (YFP−) astrocytes did not survive in our RA culture conditions (Figure 4B). Given that we observed small numbers of DCX+ SVZ derived cells en route to the lesion site post stroke, and the report by Seidenfaden et al. (2006) suggesting that neuroblasts can generate glial progeny in vivo, we sought to determine whether neuroblasts were a source of RAs in our cultures. We did this by magnetic activated cell sorting (MACS) PSA-NCAM positive cells (migratory neuroblasts) from the

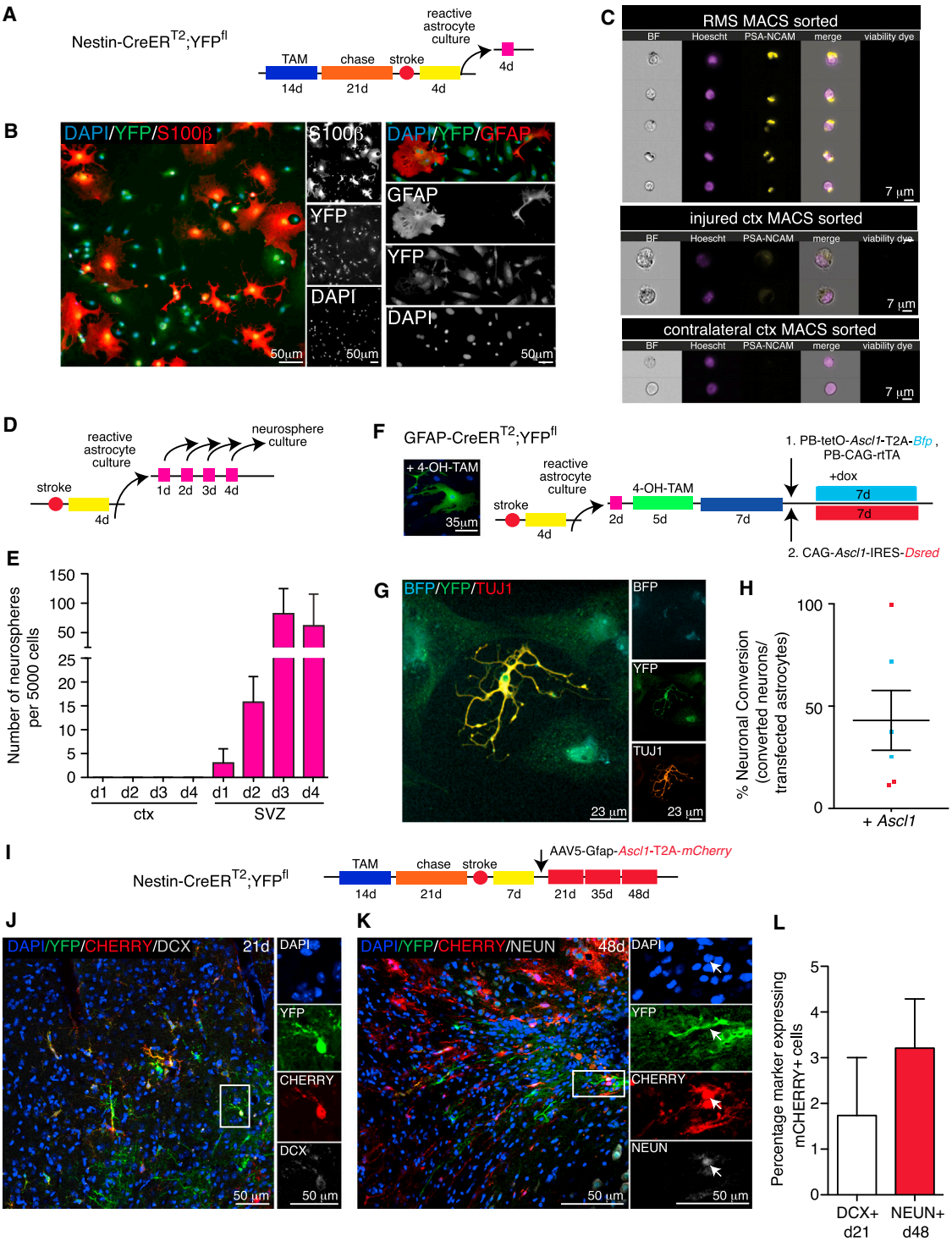

Figure 4. Forced Transcription Factor Expression Converts SVZ Derived Reactive Astrocytes to Neurons

(A) Lineage tracing of SVZ derived RAs in vitro using Nestin-CreER^{T2};YFP^{fl} mice.

(B) YFP expression in GFAP+ and S100β+ astrocytes.

(C) Pictures from ImageStream analysis of MACS sorted RMS, stroke-injured cortex, and uninjured contralateral cortex.

(D) Experimental design for assessing the presence of a residual precursor cell in RA culture conditions.

(E) Numbers of NSs derived from plating cortex and SVZ in RA conditions.

(F) Experimental design for conversion using GFAP-CreER^{T2};YFP^{fl} mice. The picture shows YFP+ astrocytes after 4-OH-TAM induced recombination.

(G) TUJ1+ neuron after expression of PB-tet-O-*Ascl1*-T2A-*Bfp* in YFP labeled astrocytes in vitro.

(legend continued on next page)

injured cortex and establishing RA cultures from the column flow through (supernatant). RA cultures could not be established from the MACS sorted fraction. To validate the MACS sort, we performed ImageStream analysis on sorted and unsorted fractions from the injured cortex, the rostral migratory stream (RMS) (to control for PSA-NCAM+ neuroblasts), and the uninjured cortex. ImageStream analysis showed the presence of PSA-NCAM+ neuroblasts with intense punctate staining (bright detail intensity) on their surface in the sorted RMS fraction (Figures 4C and S3A), but not in from the damaged cortex (Figures 4C and S3B) or the uninjured contralateral cortex (Figures 4C and S3C), consistent with no RA culture establishment from the sorted cortical fraction and the absence of dcx+ neuroblasts in the injured cortex at 4 days post injury in tissue sections. We confirmed that NS forming cells were not contaminating our RA cultures by plating cells derived from RA cultures in NS forming conditions (Figure 4D). No NSs were observed from 1-, 2-, 3-, and 4-day RA cultures (Figure 4E).

To examine whether RAs could be converted to neurons, we established RA cultures from GFAP-CreER^{T2};YFP^{fl} mice and forced expression of *Ascl1*, which alone or in combination with other factors has been successfully used to convert fibroblasts, hepatocytes, and astrocytes to neurons (Heinrich et al., 2010; Marro et al., 2011; Vierbuchen et al., 2010). We used two different transfection systems: (1) PB-tet-O-*Ascl1*-T2A-*Bfp*, and (2) CAG-*Ascl1*-IRES-*Dsred* (Figure 4F). As predicted, we found that forced expression of *Ascl1* resulted in conversion of RAs to TUJ1+ neurons (6/7 independent cultures showed successful conversion; Figure 4G), with efficiencies ranging from 11%–100% (Figure 4H). We never observed TUJ1+ neurons in control (non-transfected) cultures (0/6 cultures). TUJ1+ cells co-expressed the mature neuronal marker MAP2 (Figure S3D), indicating that SVZ derived RAs can be converted to mature neurons by forced expression of a single transcription factor, *Ascl1*.

To test the possibility of converting SVZ derived RAs to neurons using only *Ascl1* in vivo, we transduced GFAP+ RAs in tamoxifen fed and chased Nestin-CreER^{T2};YFP^{fl} mice 7 days post stroke with either an AAV5-Gfap-*Ascl1*-T2A-*mCherry* or an AAV5-Gfap-*mCherry* control (Figures 4I and S3E). This paradigm allowed us to assess conversion of GFAP+ RAs that were derived from the SVZ (YFP+). Interestingly, at 21 days post stroke, we observed rare YFP+mCHERRY+DCX+ cells (Figure 4J) and by 35 days YFP+mCHERRY+NEUN+ cells were seen within the cortex that persisted at 48 days post injury (Figure 4K). Conversion efficiencies using AAV5-Gfap-*Ascl1*-T2A-*mCherry* were 1.74 ± 1.27% at day 21 and 3.21 ± 1.1% at day 48 (Figure 4L). No NEUN+mCHERRY+ neurons were detected in AAV5-Gfap-*mCherry* transduced controls (0/4). Interesting, in vivo, *Ascl1* conversion occurs in cells close to the lesion core where the host neurons have undergone cell death. These findings indicate that *Ascl1* alone can be used to reprogram SVZ derived RAs, albeit at low efficiencies, in vivo.

DISCUSSION

Using a battery of genetic tools, we have shown that SVZ derived NSCs migrate to the damaged cortex after an injury, where a subpopulation will give rise to RAs. While previous studies (Buffo et al., 2008; Shimada et al., 2012) report de-differentiation of RAs to multipotent self-renewing cells, our work demonstrates the derivation of cortical NSs from SVZ derived precursors. Our triple transgenic paradigm allowed simultaneous tracking of SVZ precursors that express tdTOMATO activated by Nestin-CreER^{T2} prior to stroke and GFP driven by the GFAP promoter and astrocytes, which would only express GFP driven by GFAP. No GFP+ only NSs were seen, suggesting that RAs do not have the potential to form NSs after cortical injury. Rather, we show that NSCs leave their SVZ niche, migrate to the stroke-injured cortex, and retain their ability to form multipotent NSs when isolated in vitro. These findings were confirmed in the NestinCreER^{T2};YFP^{fl} mice, where recombination frequencies in the cortex were similar to what was seen in the SVZ, supporting the hypothesis that ctxNSs originated from NSC migration from the SVZ to the damaged cortex. Further, ablation of dividing cells in the SVZ eliminated ctxNS formation.

It remains to be determined whether the different findings regarding the origin of NS forming cells are due to the different injury models employed. Stroke elicits a robust response in the SVZ (Arvidsson et al., 2002) and it is not clear if a similar response is seen after stab wound injury (Synowitz et al., 2006; Tzeng and Wu, 1999). As such, the different cellular responses observed in response to injury may underlie the differences reported. Notably, cortical neurosphere formation has been reported from resident astrocytes after middle cerebral artery occlusion (MCAO) (Shimada et al., 2012; Sirko et al., 2013), a more severe form of stroke that leads to significant cortical and subcortical lesions (Popp et al., 2009). Hence, the location of the injury (cortex versus striatum) may also play a role in determining the response of cells in the SVZ. Indeed, we know from previous studies that the striatum and cortex have distinct responses to injury (Fuentealba et al., 2015; Magnusson et al., 2014; Nato et al., 2015; Petit et al., 2001; Xu et al., 2001). We purport that our findings complement the work of others (Buffo et al., 2008; Shimada et al., 2012; Sirko et al., 2013) and highlight that both the location and type of injury play a significant role in the cellular response of the brain to injury.

Further, comparing the results of our study with those reporting a different origin for ctxNSs following injury, one can consider the experimental techniques employed. For instance, previous studies that performed fate tracking of astrocytes utilized tamoxifen dependent recombination driven by Glast and Gfap

(H) Percent neuronal conversion. The blue dots represent experiments using PB-tet-O-*Ascl1*-T2A-*Bfp* (n = 3; TUJ1+YFP+BFP+ cells/YFP+BFP+ cells). The red dots represent experiments using CAG-*Ascl1*-IRES-*Dsred* (n = 3; Tuj1+YFP+DSRED+ cells/YFP+DSRED+ cells).

(I) Experimental design for in vivo conversion using Nestin-CreER^{T2};YFP^{fl} mice.

(J) DCX+ neuroblasts after expression of AAV5-Gfap-*Ascl1*-T2A-*mCherry*. The higher magnification is shown of the boxed cell.

(K) NeuN+ neurons after expression of AAV5-Gfap-*Ascl1*-T2A-*mCherry*. The higher magnification is shown of the boxed cell.

(L) Percent neuronal conversion (n = 4, mCHERRY+DCX+/mCHERRY+; n = 4 mCHERRY+NEUN+/mCHERRY+) (tamoxifen = TAM, doxycycline = dox, hydroxytamoxifen = 4-OH-TAM, cortex = ctx, rostral migratory stream = RMS, brightfield = BF, and mCherry = CHERRY). See also Figure S3.

promoters (Buffo et al., 2008; Shimada et al., 2012), both of which are expressed by NSCs in the SVZ (Pastrana et al., 2009; Platel et al., 2009). Given the considerable overlap between markers expressed by NSCs and RAs, such as nestin, GFAP, BLBP, and vimentin (Robel et al., 2011), it is possible that Glast- and Gfap-mediated Cre recombination occurred in SVZ NSCs and, thus, SVZ derived cells could have contributed to the ctxNS formation observed following stab wound or MCAO injury. The methodologies used to prelabel SVZ cells and exclude their contribution to ctxNS formation following stab wound injury or MCAO relied on prelabeling SVZ cells with lentiviral vectors (Buffo et al., 2008) and DiI labeling (Shimada et al., 2012). However, low frequency of lentiviral labeling and dilution of the DiI labeling could limit the conclusion that SVZ cells are not the source of ctxNSs following injury. Notably, our studies herein do not completely exclude the possibility that an ectopically labeled astrocyte gave rise to a ctxNS. Hence, the limitations of the paradigms employed must be considered when drawing conclusions regarding the origin of ctxNSs.

A number of studies have demonstrated that SVZ precursor cells also migrate to areas of injury in the adult brain (Arvidsson et al., 2002; Zhang et al., 2004). We use a number of methodologies including lineage tracking, transgenic mice, and ablation paradigms that permit the selective loss of NS forming cells to show that migration post stroke is not limited to progenitor cells. We performed a rigorous analysis of the well-delineated properties of stem cells, multipotentiality, and self-renewal (Potten and Loeffler, 1990), to demonstrate that SVZ derived NSCs migrate to the stroke lesion site. Further, immunohistochemistry and ImageStream analysis revealed that progenitor cells expressing DCX are not present in the stroke-injured cortex at the time when we see peak ctxNS formation. Together, these findings reveal that ctxNSs in the lesion site post stroke are derived from SVZ NSCs.

Perhaps our most interesting finding is that the NSCs that migrate to the stroke-injured cortex give rise to RAs. The SVZ derived RAs that contribute to the gliotic response at later times post injury add to the heterogeneity observed within the RA population and may play specific roles in neural repair. Indeed, a recent study points to specific roles of SVZ derived RAs in postnatal hypoxia/ischemia; SVZ derived RAs expressed higher levels of thrombospondin-4 and were responsible for proper scar formation and reduction of microvascular hemorrhaging (Benner et al., 2013). Moreover, a recent article showed no evidence for human cortical neurogenesis after stroke using carbon dating techniques (Huttner et al., 2014) and may point to an alternate role of the SVZ in producing RAs after stroke.

A number of studies have shown that developmental signaling pathways involved in early astrogliogenesis (Bauer et al., 2007; Yang et al., 2013) are reactivated post injury (Bauer et al., 2007). Further elucidation of the roles of signaling pathways such as the janus kinase/signal transducer and activator of transcription (JAK/STAT), and cytokines such as cardiotrophin-1 (CT-1), leukemia inhibitory factor (LIF), and ciliary neurotrophic factor (CNTF) (Yang et al., 2013) will lead to a clearer understanding of the subpopulations of RAs and their involvement in repair mechanisms after stroke. Further, epigenetic modifications that allow binding of transcriptional factors to astrocyte promoters and activate their expression may be the mechanism whereby cytokines exert their effect on astrocyte differentiation (Yang et al., 2013).

The "lack of success" from transplantation paradigms and endogenous neurogenesis (Dibajnia and Morshead, 2013) could be the result of astrocyte differentiation favored over neuronal differentiation. Indeed, Shimada et al. (2012) showed a loss of neurogenic potential of transplanted cortical derived neurospheres following transplantation back into the uninjured brain; only astrocytes and oligodendrocytes were produced. Nonetheless, the existence of a multipotent cell in the cortex after stroke offers the possibility of manipulating these cells for brain repair. Along these lines, *Ascl1* was reported to promote neurogenesis from NSCs (Kim et al., 2009) and astrocytes (Corti et al., 2012) and is a key regulator of fibroblast to neuron conversion in vitro (Chanda et al., 2014). We used *Ascl1* to target the progeny of SVZ derived cells and have shown that it is sufficient to convert these cells to neurons, both in vitro and in vivo. Hence, SVZ derived RAs may provide a target for neural repair. The low conversion efficiency of these cells in vivo may reflect regional/age differences in the brain, as has been suggested by recent studies targeting endogenous glia for cellular conversion (Guo et al., 2014; Heinrich et al., 2010, 2011, 2014; Niu et al., 2013; Pollak et al., 2013; Su et al., 2014). Given the cellular heterogeneity that has been reported, it is likely that cells in different regions may respond differently to transcription factors and other stimuli. Cells that migrate to the cortex, for example, may be intrinsically different or undergo different specification than those that migrate to the striatum, such that transcription factors used successfully in one brain region may not directly translate to another. Indeed, *Ascl1* is endogenously upregulated in resident astrocytes in the striatum after stroke (Magnusson et al., 2014) and has been used successfully in combination with other transcription-factors in the striatum (Torper et al., 2013). *Ascl1* alone is sufficient to convert Muller glia into neurogenic progenitors in the retina (Pollak et al., 2013). More importantly, it remains to be seen if manipulating these cells will be beneficial or detrimental to tissue regeneration in vivo. A clearer understanding of subpopulations of RAs and their involvement in repair mechanisms may help us to identify the best cell type for therapeutic cell conversion.

EXPERIMENTAL PROCEDURES

Mice

C57BL/6J and hGFAP-GFP mice (Zhuo et al., 1997) were used to assess ctxNS formation. GFAP-TK mice (Bush et al., 1998) were used for selective ablation of GFAP+ NS forming cells. For analysis of the origin of stem cells in the cortex, Nestin-CreER^{T2} mice (Imayoshi et al., 2006) were crossed with tdTomato^{fl} mice (Madisen et al., 2010) and Nestin-CreER^{T2} mice (Lagace et al., 2007) were crossed with YFP^{fl} mice (Srinivas et al., 2001), resulting in Nes-CreER^{T2};tdTomato^{fl} and Nestin-CreER^{T2};YFP^{fl} mice. Nestin-CreER^{T2};tdTomato^{fl} mice were crossed to hGFAP-GFP mice, resulting in Nestin-CreER^{T2};tdTomato^{fl};hGFAP-GFP mice. In addition, Cspg4-DsRed mice (Zhu et al., 2008) were used. For RA conversion experiments, GFAP-CrER^{T2} mice (Casper et al., 2007) were crossed to YFP^{fl} transgenic mice, resulting in GFAP-CreER^{T2};YFP^{fl} transgenic mice.

Experiments were conducted according to protocols approved by the Toronto Centre for Phenogenomics and the Department of Comparative Medicine of the University of Toronto.

ET-1 Stroke

1 μl of 400 pmolar ET-1 (Calbiochem) was injected stereotaxically into the cortex at 0.6 anterior-posterior (AP), 2.25 medial-lateral (ML), −1 dorsal-ventral (DV) (sensory-motor cortex coordinates); −1.7 AP, +4 ML, −3 DV (lateral coordinates); or −2.3 AP, +2 ML, −0.5 DV (caudal coordinates), relative to bregma.

PVD Stroke

PVD strokes were induced by removing the skull and dura in the region bound by 0.5 to +2.5 AP and +0.5 to 3 ML, relative to bregma. A saline-soaked cotton swab was used to remove pial vessels.

Tamoxifen Induction

Animals were fed tamoxifen food (0.5% TAM and 5% sucrose; Harlan) for 2 weeks followed by a chase period of 2–3 weeks.

Adeno Associated Viral Injections

1 μl of AAV5-Gfap-*Ascl1*-T2A-*mCherry* or AAV5-Gfap-*mCherry* particles (VectorBioLabs) were injected into the cortex of NestinCreER^{T2};YFP^{fl} mice 7 days post stroke.

NS Culture

NSs were cultured as previously described (Coles-Takabe et al., 2008; Tropepe et al., 1997). Cells were plated at clonal density (5 cells/μL).

RA Culture and Conversion

The cortex was dissected from GFAP-CreER^{T2};YFP^{fl} mice. Cells were plated in astrocyte media with 1 mM 4-OH-TAM. After 7 days, cells were transfected with PBase, PB-CAG-rtTA (Woltjen et al., 2009), and PB−tetO-*Ascl1*-T2A-*Bfp* or CAG-*Ascl1*-IRES-*Dsred* using HD Fugene (Roche). The media was changed to N2B27. For PB−tetO-*Ascl1*-T2A-*Bfp* expression, 1,500 ng/mL dox was added.

MACS and ImageStream Analysis

Cells were stained with anti-PSA-NCAM-PE (Miltenyi Biotech) and MACS sorted. For ImageStream analysis, cells were stained with a fixable cell viability dye (FVD eFluor 780; eBioscience), anti-PSA-NCAM-PE (Miltenyi Biotech), or a mouse IgM-PE control (Miltenyi Biotech), MACS sorted and stained with Hoescht (BD Biosciences). Cells were analyzed with an Amnis ImageStreamTM Mark II imaging flow cytometer (Amnis) and compensated image files were analyzed using IDEAS analysis software (Amnis).

Statistical Analysis

All experiments were conducted blind, using a numbering system. F tests were used to compare variance between groups. Unpaired two-tailed t tests or unpaired two-tailed t tests with Welch's correction (for unequal variance) were used for comparisons between two groups. A one-factor ANOVA was used followed by post hoc analysis (Tukey's or Dunnet's test) for comparisons between three or more groups. Comparison of percentages between groups was done using two sample z-tests for individual proportions. Differences were considered significant at $p < 0.05$. Values are presented as mean ± SEM.

SUPPLEMENTAL INFORMATION

Supplemental Information includes Supplemental Experimental Procedures, three figures, and one table and can be found with this article online at http://dx.doi.org/10.1016/j.stem.2015.08.002.

ACKNOWLEDGMENTS

The authors are grateful to M. Puri for critical reading of the manuscript and M. Götz for both critical reading of the manuscript and plasmids CAG-*Ascl1*-IRES-*Dsred* and CAG-*Dsred.* ImageStream analysis was done at the Lunenfeld-Tanenbaum Research Institute Flow Cytometry Core Facility. M.F. was supported by the Canadian Institute of Health Research (CIHR) postdoctoral fellowship 224002. This work was supported by grants to A.N. from the Ontario Research Fund Global Leadership Round in Genomics and Life Sciences (GL2) Stem Cell Network (9/5254 (TR3)) and CIHR (MOP 1025) and operating grants to C.M.M from CIHR (MOP 126198) and the Canadian Heart and Stroke Foundation.

Received: June 29, 2014
Revised: April 15, 2015
Accepted: August 2, 2015
Published: October 8, 2015

REFERENCES

Arvidsson, A., Collin, T., Kirik, D., Kokaia, Z., and Lindvall, O. (2002). Neuronal replacement from endogenous precursors in the adult brain after stroke. Nat. Med. *8*, 963–970.

Bauer, S., Kerr, B.J., and Patterson, P.H. (2007). The neuropoietic cytokine family in development, plasticity, disease and injury. Nat. Rev. Neurosci. *8*, 221–232.

Benner, E.J., Luciano, D., Jo, R., Abdi, K., Paez-Gonzalez, P., Sheng, H., Warner, D.S., Liu, C., Eroglu, C., and Kuo, C.T. (2013). Protective astrogenesis from the SVZ niche after injury is controlled by Notch modulator Thbs4. Nature *497*, 369–373.

Buffo, A., Rite, I., Tripathi, P., Lepier, A., Colak, D., Horn, A.P., Mori, T., and Götz, M. (2008). Origin and progeny of reactive gliosis: A source of multipotent cells in the injured brain. Proc. Natl. Acad. Sci. USA *105*, 3581–3586.

Burda, J.E., and Sofroniew, M.V. (2014). Reactive gliosis and the multicellular response to CNS damage and disease. Neuron *81*, 229–248.

Bush, T.G., Savidge, T.C., Freeman, T.C., Cox, H.J., Campbell, E.A., Mucke, L., Johnson, M.H., and Sofroniew, M.V. (1998). Fulminant jejuno-ileitis following ablation of enteric glia in adult transgenic mice. Cell *93*, 189–201.

Bush, T.G., Puvanachandra, N., Horner, C.H., Polito, A., Ostenfeld, T., Svendsen, C.N., Mucke, L., Johnson, M.H., and Sofroniew, M.V. (1999). Leukocyte infiltration, neuronal degeneration, and neurite outgrowth after ablation of scar-forming, reactive astrocytes in adult transgenic mice. Neuron *23*, 297–308.

Casper, K.B., Jones, K., and McCarthy, K.D. (2007). Characterization of astrocyte-specific conditional knockouts. Genesis *45*, 292–299.

Chanda, S., Ang, C.E., Davila, J., Pak, C., Mall, M., Lee, Q.Y., Ahlenius, H., Jung, S.W., Südhof, T.C., and Wernig, M. (2014). Generation of induced neuronal cells by the single reprogramming factor ASCL1. Stem Cell Reports *3*, 282–296.

Clarke, S.R., Shetty, A.K., Bradley, J.L., and Turner, D.A. (1994). Reactive astrocytes express the embryonic intermediate neurofilament nestin. Neuroreport *5*, 1885–1888.

Coles-Takabe, B.L., Brain, I., Purpura, K.A., Karpowicz, P., Zandstra, P.W., Morshead, C.M., and van der Kooy, D. (2008). Don't look: growing clonal versus nonclonal neural stem cell colonies. Stem Cells *26*, 2938–2944.

Corti, S., Nizzardo, M., Simone, C., Falcone, M., Donadoni, C., Salani, S., Rizzo, F., Nardini, M., Riboldi, G., Magri, F., et al. (2012). Direct reprogramming of human astrocytes into neural stem cells and neurons. Exp. Cell Res. *318*, 1528–1541.

Dibajnia, P., and Morshead, C.M. (2013). Role of neural precursor cells in promoting repair following stroke. Acta Pharmacol. Sin. *34*, 78–90.

Doetsch, F., García-Verdugo, J.M., and Alvarez-Buylla, A. (1999). Regeneration of a germinal layer in the adult mammalian brain. Proc. Natl. Acad. Sci. USA *96*, 11619–11624.

Erlandsson, A., Lin, C.H., Yu, F., and Morshead, C.M. (2011). Immunosuppression promotes endogenous neural stem and progenitor cell migration and tissue regeneration after ischemic injury. Exp. Neurol. *230*, 48–57.

Fuentealba, L.C., Rompani, S.B., Parraguez, J.I., Obernier, K., Romero, R., Cepko, C.L., and Alvarez-Buylla, A. (2015). Embryonic origin of postnatal neural stem cells. Cell *161*, 1644–1655.

Guo, Z., Zhang, L., Wu, Z., Chen, Y., Wang, F., and Chen, G. (2014). In vivo direct reprogramming of reactive glial cells into functional neurons after brain injury and in an Alzheimer's disease model. Cell Stem Cell *14*, 188–202.

Heinrich, C., Blum, R., Gascón, S., Masserdotti, G., Tripathi, P., Sánchez, R., Tiedt, S., Schroeder, T., Götz, M., and Berninger, B. (2010). Directing astroglia from the cerebral cortex into subtype specific functional neurons. PLoS Biol. *8*, e1000373.

Heinrich, C., Gascón, S., Masserdotti, G., Lepier, A., Sanchez, R., Simon-Ebert, T., Schroeder, T., Götz, M., and Berninger, B. (2011). Generation of subtype-specific neurons from postnatal astroglia of the mouse cerebral cortex. Nat. Protoc. *6*, 214–228.

Heinrich, C., Bergami, M., Gascón, S., Lepier, A., Viganò, F., Dimou, L., Sutor, B., Berninger, B., and Götz, M. (2014). Sox2-mediated conversion of NG2 glia into induced neurons in the injured adult cerebral cortex. Stem Cell Reports *3*, 1000–1014.

Hua, R., and Walz, W. (2006). Minocycline treatment prevents cavitation in rats after a cortical devascularizing lesion. Brain Res. *1090*, 172–181.

Huttner, H.B., Bergmann, O., Salehpour, M., Rácz, A., Tatarishvili, J., Lindgren, E., Csonka, T., Csiba, L., Hortobágyi, T., Méhes, G., et al. (2014). The age and genomic integrity of neurons after cortical stroke in humans. Nat. Neurosci. *17*, 801–803.

Imayoshi, I., Ohtsuka, T., Metzger, D., Chambon, P., and Kageyama, R. (2006). Temporal regulation of Cre recombinase activity in neural stem cells. Genesis *44*, 233–238.

Imura, T., Kornblum, H.I., and Sofroniew, M.V. (2003). The predominant neural stem cell isolated from postnatal and adult forebrain but not early embryonic forebrain expresses GFAP. J. Neurosci. *23*, 2824–2832.

Kim, H.J., McMillan, E., Han, F., and Svendsen, C.N. (2009). Regionally specified human neural progenitor cells derived from the mesencephalon and forebrain undergo increased neurogenesis following overexpression of ASCL1. Stem Cells *27*, 390–398.

Kolb, B., Morshead, C., Gonzalez, C., Kim, M., Gregg, C., Shingo, T., and Weiss, S. (2007). Growth factor-stimulated generation of new cortical tissue and functional recovery after stroke damage to the motor cortex of rats. J. Cereb. Blood Flow Metab. *27*, 983–997.

Lagace, D.C., Whitman, M.C., Noonan, M.A., Ables, J.L., DeCarolis, N.A., Arguello, A.A., Donovan, M.H., Fischer, S.J., Farnbauch, L.A., Beech, R.D., et al. (2007). Dynamic contribution of nestin-expressing stem cells to adult neurogenesis. J. Neurosci. *27*, 12623–12629.

Leong, S.Y., and Turnley, A.M. (2011). Regulation of adult neural precursor cell migration. Neurochem. Int. *59*, 382–393.

Lois, C., and Alvarez-Buylla, A. (1994). Long-distance neuronal migration in the adult mammalian brain. Science *264*, 1145–1148.

Madisen, L., Zwingman, T.A., Sunkin, S.M., Oh, S.W., Zariwala, H.A., Gu, H., Ng, L.L., Palmiter, R.D., Hawrylycz, M.J., Jones, A.R., et al. (2010). A robust and high-throughput Cre reporting and characterization system for the whole mouse brain. Nat. Neurosci. *13*, 133–140.

Magnusson, J.P., Göritz, C., Tatarishvili, J., Dias, D.O., Smith, E.M., Lindvall, O., Kokaia, Z., and Frisén, J. (2014). A latent neurogenic program in astrocytes regulated by Notch signaling in the mouse. Science *346*, 237–241.

Marro, S., Pang, Z.P., Yang, N., Tsai, M.C., Qu, K., Chang, H.Y., Südhof, T.C., and Wernig, M. (2011). Direct lineage conversion of terminally differentiated hepatocytes to functional neurons. Cell Stem Cell *9*, 374–382.

Molofsky, A.V., Krencik, R., Ullian, E.M., Tsai, H.H., Deneen, B., Richardson, W.D., Barres, B.A., and Rowitch, D.H. (2012). Astrocytes and disease: a neurodevelopmental perspective. Genes Dev. *26*, 891–907.

Morshead, C.M., Reynolds, B.A., Craig, C.G., McBurney, M.W., Staines, W.A., Morassutti, D., Weiss, S., and van der Kooy, D. (1994). Neural stem cells in the adult mammalian forebrain: a relatively quiescent subpopulation of subependymal cells. Neuron *13*, 1071–1082.

Morshead, C.M., Garcia, A.D., Sofroniew, M.V., and van Der Kooy, D. (2003). The ablation of glial fibrillary acidic protein-positive cells from the adult central nervous system results in the loss of forebrain neural stem cells but not retinal stem cells. Eur. J. Neurosci. *18*, 76–84.

Nato, G., Caramello, A., Trova, S., Avataneo, V., Rolando, C., Taylor, V., Buffo, A., Peretto, P., and Luzzati, F. (2015). Striatal astrocytes produce neuroblasts in an excitotoxic model of Huntington's disease. Development *142*, 840–845.

Niu, W., Zang, T., Zou, Y., Fang, S., Smith, D.K., Bachoo, R., and Zhang, C.L. (2013). In vivo reprogramming of astrocytes to neuroblasts in the adult brain. Nat. Cell Biol. *15*, 1164–1175.

Pastrana, E., Cheng, L.C., and Doetsch, F. (2009). Simultaneous prospective purification of adult subventricular zone neural stem cells and their progeny. Proc. Natl. Acad. Sci. USA *106*, 6387–6392.

Petit, A., Pierret, P., Vallée, A., and Doucet, G. (2001). Astrocytes from cerebral cortex or striatum attract adult host serotoninergic axons into intrastriatal ventral mesencephalic co-grafts. J. Neurosci. *21*, 7182–7193.

Platel, J.C., Gordon, V., Heintz, T., and Bordey, A. (2009). GFAP-GFP neural progenitors are antigenically homogeneous and anchored in their enclosed mosaic niche. Glia *57*, 66–78.

Pollak, J., Wilken, M.S., Ueki, Y., Cox, K.E., Sullivan, J.M., Taylor, R.J., Levine, E.M., and Reh, T.A. (2013). ASCL1 reprograms mouse Muller glia into neurogenic retinal progenitors. Development *140*, 2619–2631.

Popp, A., Jaenisch, N., Witte, O.W., and Frahm, C. (2009). Identification of ischemic regions in a rat model of stroke. PLoS ONE *4*, e4764.

Potten, C.S., and Loeffler, M. (1990). Stem cells: attributes, cycles, spirals, pitfalls and uncertainties. Lessons for and from the crypt. Development *110*, 1001–1020.

Robel, S., Berninger, B., and Götz, M. (2011). The stem cell potential of glia: lessons from reactive gliosis. Nat. Rev. Neurosci. *12*, 88–104.

Seidenfaden, R., Desoeuvre, A., Bosio, A., Virard, I., and Cremer, H. (2006). Glial conversion of SVZ-derived committed neuronal precursors after ectopic grafting into the adult brain. Mol. Cell. Neurosci. *32*, 187–198.

Shimada, I.S., LeComte, M.D., Granger, J.C., Quinlan, N.J., and Spees, J.L. (2012). Self-renewal and differentiation of reactive astrocyte-derived neural stem/progenitor cells isolated from the cortical peri-infarct area after stroke. J. Neurosci. *32*, 7926–7940.

Sirko, S., Behrendt, G., Johansson, P.A., Tripathi, P., Costa, M., Bek, S., Heinrich, C., Tiedt, S., Colak, D., Dichgans, M., et al. (2013). Reactive glia in the injured brain acquire stem cell properties in response to sonic hedgehog. [corrected]. Cell Stem Cell *12*, 426–439.

Srinivas, S., Watanabe, T., Lin, C.S., William, C.M., Tanabe, Y., Jessell, T.M., and Costantini, F. (2001). Cre reporter strains produced by targeted insertion of EYFP and ECFP into the ROSA26 locus. BMC Dev. Biol. *1*, 4.

Su, Z., Niu, W., Liu, M.L., Zou, Y., and Zhang, C.L. (2014). In vivo conversion of astrocytes to neurons in the injured adult spinal cord. Nat. Commun. *5*, 3338.

Sun, M.Y., Yetman, M.J., Lee, T.C., Chen, Y., and Jankowsky, J.L. (2014). Specificity and efficiency of reporter expression in adult neural progenitors vary substantially among nestin-CreER(T2) lines. J. Comp. Neurol. *522*, 1191–1208.

Synowitz, M., Kiwit, J., Kettenmann, H., and Glass, R. (2006). Tumor Young Investigator Award: tropism and antitumorigenic effect of endogenous neural precursors for gliomas. Clin. Neurosurg. *53*, 336–344.

Torper, O., Pfisterer, U., Wolf, D.A., Pereira, M., Lau, S., Jakobsson, J., Björklund, A., Grealish, S., and Parmar, M. (2013). Generation of induced neurons via direct conversion in vivo. Proc. Natl. Acad. Sci. USA *110*, 7038–7043.

Tropepe, V., Craig, C.G., Morshead, C.M., and van der Kooy, D. (1997). Transforming growth factor-alpha null and senescent mice show decreased neural progenitor cell proliferation in the forebrain subependyma. J. Neurosci. *17*, 7850–7859.

Tzeng, S.F., and Wu, J.P. (1999). Responses of microglia and neural progenitors to mechanical brain injury. Neuroreport *10*, 2287–2292.

Vierbuchen, T., Ostermeier, A., Pang, Z.P., Kokubu, Y., Südhof, T.C., and Wernig, M. (2010). Direct conversion of fibroblasts to functional neurons by defined factors. Nature *463*, 1035–1041.

Wanner, I.B., Anderson, M.A., Song, B., Levine, J., Fernandez, A., Gray-Thompson, Z., Ao, Y., and Sofroniew, M.V. (2013). Glial scar borders are formed by newly proliferated, elongated astrocytes that interact to corral inflammatory and fibrotic cells via STAT3-dependent mechanisms after spinal cord injury. J. Neurosci. *33*, 12870–12886.

Woltjen, K., Michael, I.P., Mohseni, P., Desai, R., Mileikovsky, M., Hämäläinen, R., Cowling, R., Wang, W., Liu, P., Gertsenstein, M., et al. (2009). piggyBac transposition reprograms fibroblasts to induced pluripotent stem cells. Nature *458*, 766–770.

Xu, L., Sapolsky, R.M., and Giffard, R.G. (2001). Differential sensitivity of murine astrocytes and neurons from different brain regions to injury. Exp. Neurol. *169*, 416–424.

Yang, Y., Higashimori, H., and Morel, L. (2013). Developmental maturation of astrocytes and pathogenesis of neurodevelopmental disorders. J. Neurodev. Disord. *5*, 22.

Zhang, R., Zhang, Z., Wang, L., Wang, Y., Gousev, A., Zhang, L., Ho, K.L., Morshead, C., and Chopp, M. (2004). Activated neural stem cells contribute to stroke-induced neurogenesis and neuroblast migration toward the infarct boundary in adult rats. J. Cereb Blood Flow Metab. *24*, 441–448.

Zhu, X., Bergles, D.E., and Nishiyama, A. (2008). NG2 cells generate both oligodendrocytes and gray matter astrocytes. Development *135*, 145–157.

Zhuo, L., Sun, B., Zhang, C.L., Fine, A., Chiu, S.Y., and Messing, A. (1997). Live astrocytes visualized by green fluorescent protein in transgenic mice. Dev. Biol. *187*, 36–42.

Cell Stem Cell

Supplemental Information

Adult Neural Stem Cells from the Subventricular Zone Give Rise to Reactive Astrocytes in the Cortex after Stroke

Maryam Faiz, Nadia Sachewsky, Sergio Gascón, K.W. Annie Bang, Cindi M. Morshead, and Andras Nagy

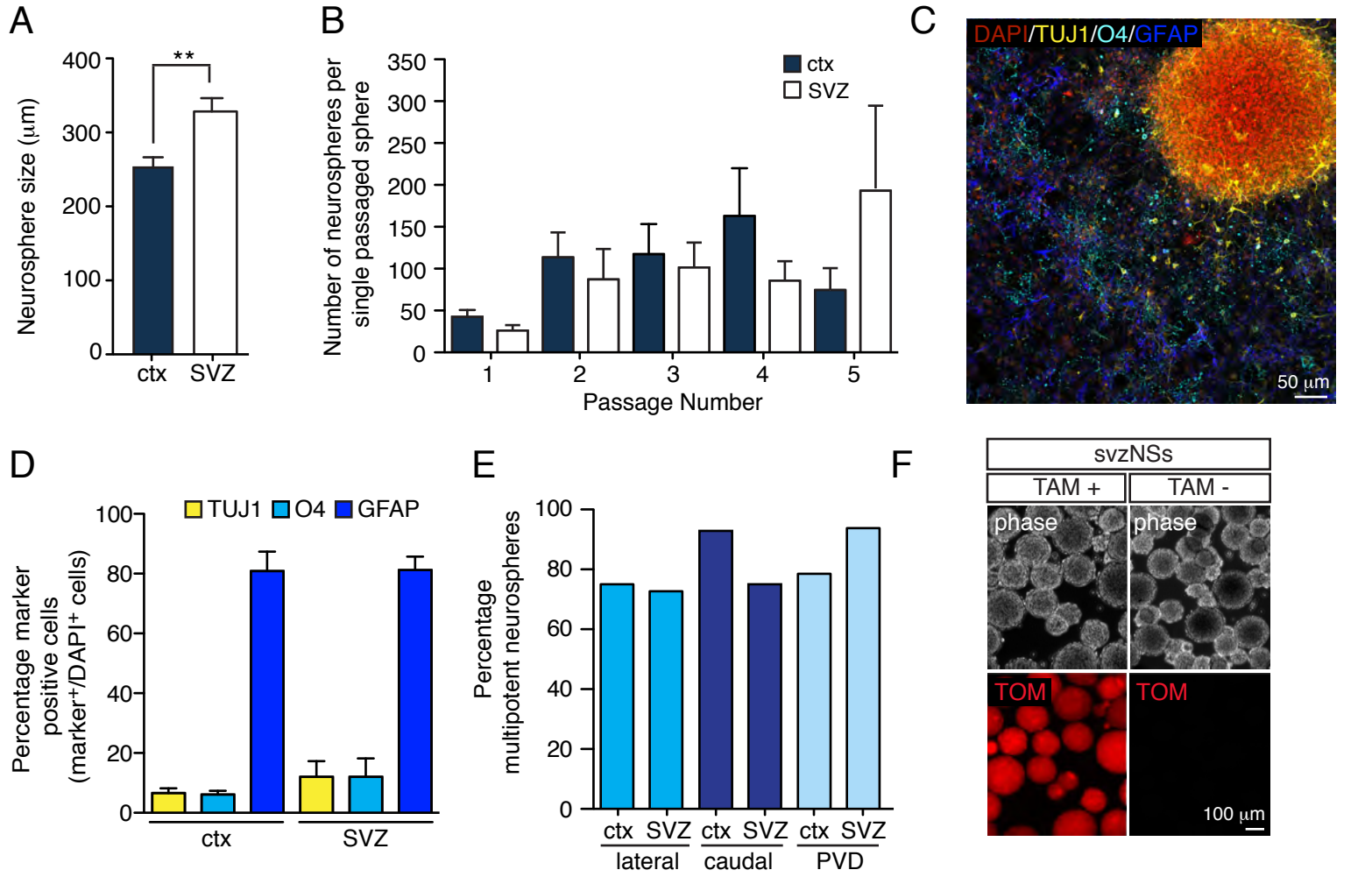
A
Neurosphere size (μm)
400
300
200
100
0
**
ctx
SVZ
B
Number of neurospheres per single passaged sphere
350
300
250
200
150
100
50
0
ctx
SVZ
1
2
3
4
5
Passage Number
C
DAPI/TUJ1/O4/GFAP
50 μm
D
Percentage marker positive cells (marker+/DAPI+ cells)
TUJ1
O4
GFAP
100
80
60
40
20
0
ctx
SVZ
E
Percentage multipotent neurospheres
100
80
60
40
20
0
ctx SVZ ctx SVZ ctx SVZ
lateral
caudal
PVD
F
svzNSs
TAM +
TAM -
phase
phase
TOM
TOM
100 μm

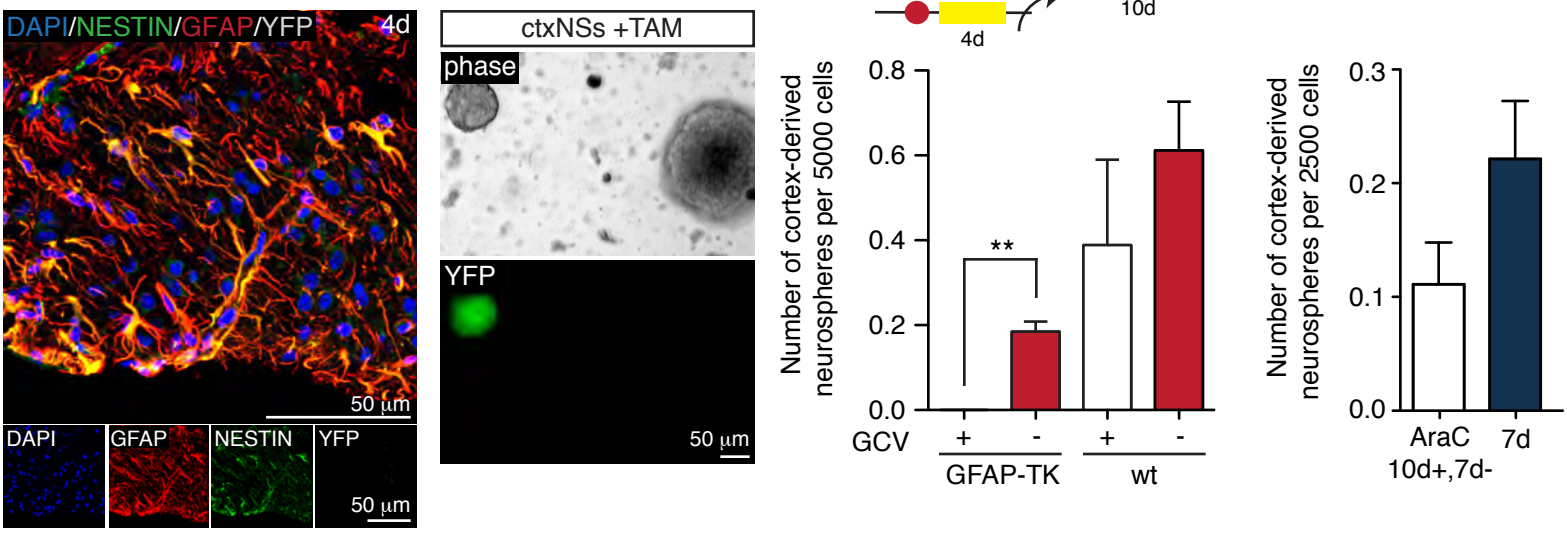
G
DAPI/NESTIN/GFAP/YFP
4d
50 μm
DAPI
GFAP
NESTIN
YFP
50 μm
H
ctxNSs +TAM
phase
YFP
50 μm
I
stroke
4d
neurosphere culture
GCV
10d
Number of cortex-derived neurospheres per 5000 cells
0.8
0.6
0.4
0.2
0.0
**
GCV
+
-
+
-
GFAP-TK
wt
J
Number of cortex-derived neurospheres per 2500 cells
0.3
0.2
0.1
0.0
AraC
7d
10d+,7d-

Figure S1

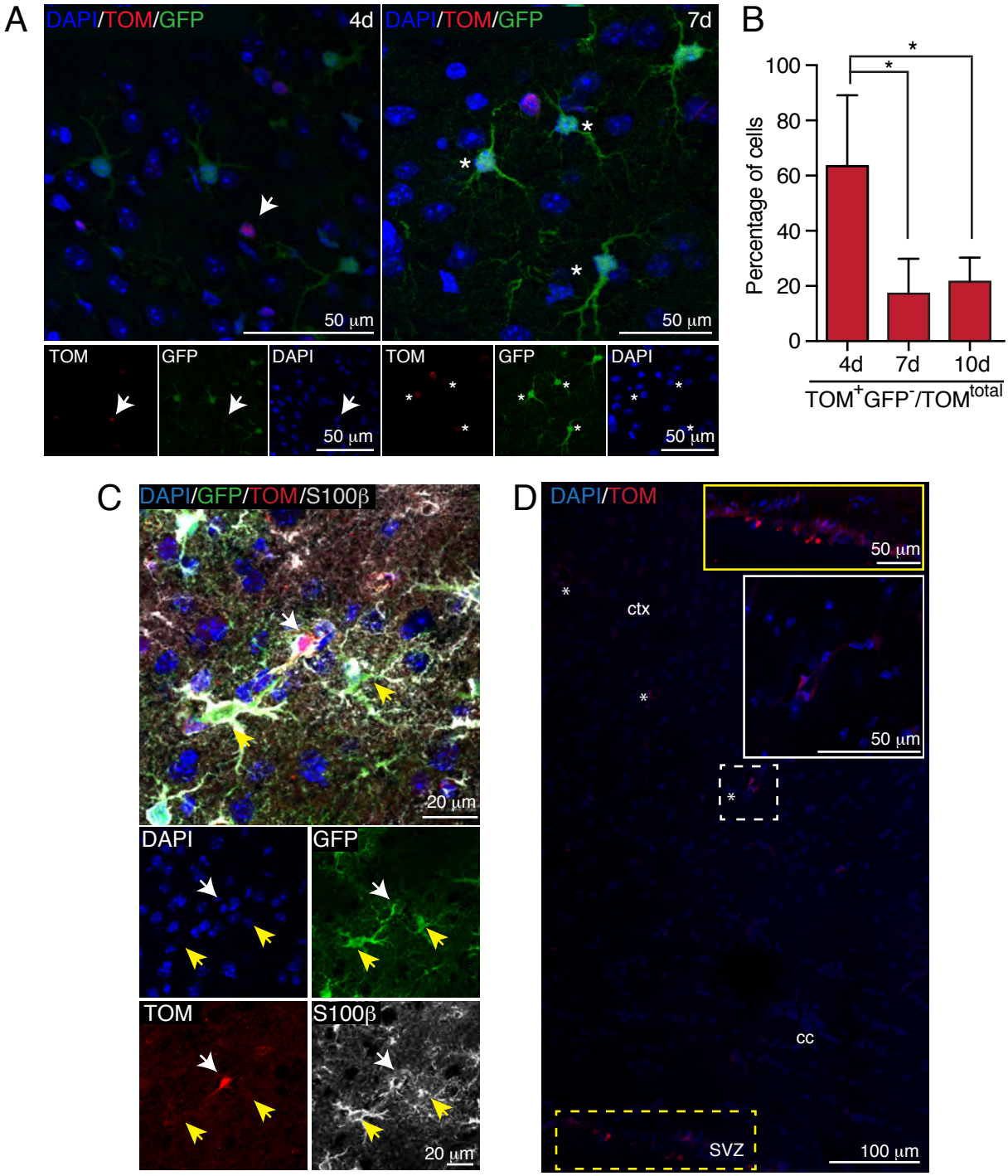
A
DAPI/TOM/GFP
4d
DAPI/TOM/GFP
7d
50 μm
50 μm
TOM
GFP
DAPI
50 μm
TOM
GFP
DAPI
50 μm
B
Percentage of cells
100
80
60
40
20
0
4d
7d
10d
TOM+GFP-/TOMtotal
C
DAPI/GFP/TOM/S100β
20 μm
DAPI
GFP
TOM
S100β
20 μm
D
DAPI/TOM
50 μm
ctx
50 μm
cc
SVZ
100 μm

Figure S2

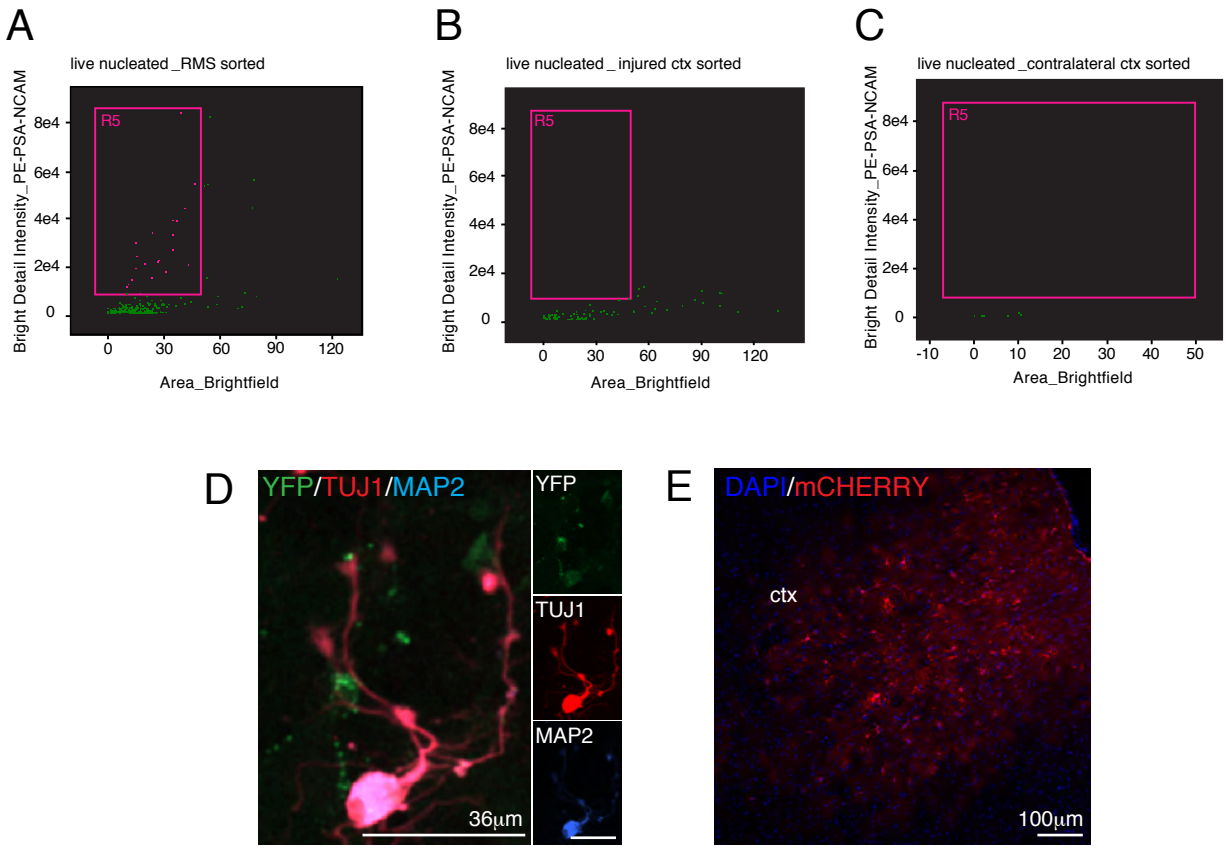
A
live nucleated _RMS sorted
Bright Detail Intensity_PE-PSA-NCAM
R5
8e4
6e4
4e4
2e4
0
0
30
60
90
120
Area_Brightfield
B
live nucleated _ injured ctx sorted
Bright Detail Intensity_PE-PSA-NCAM
R5
8e4
6e4
4e4
2e4
0
0
30
60
90
120
Area_Brightfield
C
live nucleated _contralateral ctx sorted
Bright Detail Intensity_PE-PSA-NCAM
R5
8e4
6e4
4e4
2e4
0
-10
0
10
20
30
40
50
Area_Brightfield
D
YFP/TUJ1/MAP2
YFP
TUJ1
MAP2
36μm
E
DAPI/mCHERRY
ctx
100μm

Figure S3

Table S1, Related to Figure 1. Percentage YFP+ labeled neurospheres from the SVZ and cortex of NesCreER^{T2};YFP^{fl} mice

Animal #	% Labeled YFP+ svzNSs	% Labeled YFP+ ctxNSs
1	3%	7% (1 of 15)
2	3%	4% (1 of 16)
3	4%	9% (1 of 11)
4	6%	6% (1 of 17)
5	7%	7% (1 of 14)
6	7%	7% (3 of 44)
7	8%	8% (1 of 12)
8	8%	5% (1 of 19)
9	9%	16% (1 of 6)
10	22%	43% (3 of 7)
11	28%	33% (1 of 3)
12	50%	100% (1 of 1)

Supplemental Figure Legends

Figure S1, Related to Figure 1. Neurospheres derived from the stroke-injured cortex

(A) Size of ctxNSs (** =p=0.0011, unpaired *t* test with Welch's correction, t(135) = 3.343, data represent ± s.e.m., n_{cx} = 71, n_{SVZ} =72, 4 independent trials). (B) Number of neurospheres from individual clones at each passage (n.s., unpaired *t* test with Welch's correction (except passage 2), $t(75)_{passage1}$ = 1.528, $t(71)_{passage2}$ = 0.4922, $t(55)_{passage3}$ = 0.3393, $t(31)_{passage4}$ = 1.254, $t(19)_{passage5}$ = 1.161 data represent ± s.e.m., n_{P1cx} = 73, n_{P2cx} = 39, n_{P3cx} = 49, n_{P4cx} = 27, n_{P5cx} = 9, n_{P1SVZ} = 17, n_{P2SVZ} = 16, n_{P3SVZ} = 16, n_{P4SVZ} = 16, n_{P5SVZ} = 16, 4 independent trials). (C) Multipotent sphere with TUJ1+ neurons, O4+ oligodendrocytes and GFAP+ astrocytes. (D) Percentage of neurons, astrocytes and oligodendrocytes upon differentiation (n.s. unpaired *t* test, $t(18)_{Tuj1}$ = 1.325, $t(17)_{O4}$ = 1.4225, $t(8)_{GFAP}$ = 0.02691, data represent ± s.e.m. from n_{Tuj1_cx} = 16, n_{Tuj1_SVZ} = 4; n_{Tuj1_cx} = 13, n_{Tuj1_SVZ} = 6; n_{O4_cx} = 7, n_{O4_SVZ} = 3, 3 independent trials). (E) Percent multipotent neurospheres formed from the cortex after lesions at sites lateral and caudal to the original injury of the sensory-motor cortex and from the cortex after pial vessel disruption (PVD) (ns = p_{PVD} = 0.18684, $p_{lateral}$ = 0.90448 = p_{caudal} = 0.31732 Z-test for independent proportions, z_{PVD} = -1.3242 $z_{lateral}$ = 0.124, z_{caudal} = 1.0022, data represent $n_{lateral\_ctx\_}$ = 11, $n_{lateral\_SVZ}$ = 12, n_{caudal_ctx} = 4, , n_{caudal_SVZ} = 14, n_{PVD_ctx} = 16, n_{PVD_SVZ} = 28. (F) tdTOMATO expression in svzNSs from tamoxifen fed and unfed mice. (G) NESTIN expression in YFP-GFAP+ astrocytes 4d after

stroke. (H) YFP expression in ctxNSs from tamoxifen fed mice. (I) GCV ablation paradigm and number of cortex-derived neurospheres after GCV administration in wt and GFAP-TK mice (**=p= 0.0015, paired *t* test, t(4) = 7.770, data represent ± s.e.m. from n_{wt_+GCV} = 5, n_{wt_-GCV} = 5; n.s. = p= 0.3503, paired *t* test, t(5) = 1.030, data represent ± s.e.m. from $n_{GFAP\text{-}TK\_+GCV}$ = 6, $n_{GFAP\text{-}TK\_-GCV}$ = 6. (J) Number of ctxNSs at 7d and 7d after AraC ablation (n.s., unpaired *t* test, t (9) = 1.857, data represent ± s.e.m. from $n_{10dAraC\_7d}$ = 4, n_{7d} = 7. SVZ = subventricular zone, cc = corpus callosum, ctx = cortex, lv = lateral ventricle, PVD = pial vessel disruption, TAM = tamoxifen, TOM = tdTomato.

Figure S2, Related to Figure 3. SVZ-derived cells differentiate into reactive astrocytes in the cortex after stroke.

(A) tdTOMATO+ and GFP+ cells at 4d and 7d post stroke. White arrow shows a tdTomato+GFP- cell, white asterisks show tdTOMATO+GFP+ cells. (B) Ratio of SVZ-derived precursors ($TOM+GFP+/TOM^{total}$) in Nestin-$CreER^{T2}$;$tdTomato^{fl}$;hGFAP-GFP mice (* = p<0.05, One-way ANOVA with Tukey's post hoc, $F(3,10)_{Tom+GFP-\ /Tom^{total}+}$ = 8.442, F(3,10) data represent ± s.e.m., n_{4d} = 3, n_{7d} = 4, n_{10d} = 4). (C) S100β expression in tdTOMATO+GFP+ reactive astrocyte. White arrowheads show tdTOMATO+GFP+S100β+ positive cell, yellow arrowheads show tdTOMATO-GFP+S100β+ cells. (D) tdTOMATO expression in uninjured tamoxifen fed mice. White and yellow insets show higher magnification photos of regions in dashed white and yellow boxes, asterisks

show labeling of vasculature. ctx = cortex, cc = corpus callosum, DCX = doublecortin, SVZ = subventricular zone, TOM = tdTomato.

Figure S3, Related to Figure 4. Conversion of reactive astrocytes to neurons

(A) ImageStream plot of the MACS sorted RMS. Gated cells in R5 show punctate PSA-NCAM on the surface of cells in the RMS. (B) ImageStream plot of the MACS sorted injured cortex. (C) ImageStream plot of the MACS sorted uninjured contralateral cortex. (D) TUJ1+MAP2+ neuron converted from a YFP labeled astrocyte. (E) mCHERRY expression in the cortex after AAV5-Gfap-*Ascl1*-T2A–*mCherry* injection. ctx = cortex

Table S1, Related to Figure 1. Percentage YFP+ labeled neurospheres from the SVZ and cortex of NesCreER^{T2};YFP^{fl} mice.

Numbers represent the percentage of YFP labeled neurospheres in the SVZ (svzNSs) and cortex (ctxNSs) per animal.

Supplemental Experimental Procedures

Mice

For NS analysis of cortex-derived versus SVZ-derived NSs at various times post stroke, C57BL/6J or hGFAP^{promoter}-GFP (hGFAP-GFP; Jackson Labs: FVB/N-Tg(GFAPGFP)14Mes/J) transgenic mice (Zhuo et al., 1997) were used.

No differences were found between strains regarding neurosphere number, size, passaging and differentiation.

For selective ablation of GFAP+ neurosphere forming cells, GFAP^{promoter}-TK (GFAP-TK; Jackson Labs: B6.Cg-Tg(Gfap-TK)7.1Mvs/J) mice (Bush et al., 1998) were used.

For analysis of the origin of stem cells in the cortex post stroke, Nestin^{promoter}-CreER^{T2} (Nestin-CreER^{T2}) transgenic mice (Imayoshi et al., 2006) were crossed with Rosa26-loxP-stop-loxP-tdTomato (tdTomato^{fl}; Jackson Labs: B6;129S6-*Gt(ROSA)26Sortm9(CAG-tdTomato)Hze*/J) transgenic reporter mice (Madisen et al., 2010) and Nestin-CreER^{T2} mice (Lagace et al., 2007) were crossed with Rosa26-loxP-stop-loxP-YFP (YFP^{fl}; Jackson Labs: B6.129X1-*Gt(ROSA)26Sortm1(EYFP)Cos*/J) transgenic reporter mice (Srinivas et al., 2001), resulting in Nes-CreER^{T2};tdTomato^{fl} and Nestin-CreER^{T2};YFP^{fl} double transgenic mice. Nestin-CreER^{T2};tdTomato^{fl} mice were crossed to hGFAP-GFP mice, resulting Nestin-CreER^{T2};tdTomato^{fl};hGFAP-GFP triple transgenic mice. In addition, Cspg4^{promoter}-DsRed (Cspg4-DsRed; Jackson Labs: Tg(Cspg4-DsRed.T1)1Akik) mice (Zhu et al., 2008) were used.

To assess conversion of reactive astrocytes to neurons GFAP^{promoter}-CreER^{T2} (GFAP-CrER^{T2}; Jackson Labs: Tg(GFAP-cre/ERT2)13Kdmc) mice (Casper et al., 2007) were crossed to YFP^{fl} transgenic mice, resulting in GFAP-CreER^{T2};YFP^{fl} transgenic mice.

Both males and females aged 6 weeks – 5 months were included in the analysis. All mice were housed in a barrier facility with a 12 hour light/12 hour dark cycle and allowed free access to food and water with a maximum of 4 mice per cage. Experiments were conducted according to protocols approved by the Toronto Center for Phenogenomics and the Department of Comparative Medicine of the University of Toronto.

Endothelin-1 stroke

Endothelin-1 (ET-1) strokes were preformed similar to as previously described (Tennant and Jones, 2009). One μL of 400 picomolar endothelin-1 (ET-1, Calbiochem) was injected streotaxically into the cortex at 0.6 AP, 2.25 ML, -1 DV (sensory-motor cortex coordinates), -1.7 AP, +4 ML, -3 DV (lateral coordinates) or -2.3 AP, +2 ML, -0.5 DV (caudal coordinates), relative to bregma. A 26 gauge Hamilton syringe with a 45 degree beveled tip was used to inject ET-1 at a rate of 0.1ml/min. The needle was left in place for 10 minutes after ET-1 injection to prevent backflow and then slowly withdrawn.

PVD stroke

PVD strokes were induced by removing the skull and dura in the region bound by 0.5 to +2.5 AP, +0.5 to 3 ML, relative to bregma. A saline-soaked cotton swab was used to remove pial vessels.

Cytosine b-D-arabinoside (AraC) infusion

For AraC infusion, a cannula was implanted to target the lateral ventricle (0.2 AP, 0.8 ML, and 2.5 DV, relative to bregma) and connected to a subcutaneous mini-osmotic pump (1007D, Alzet; 0.5μl/hour) overlying the shoulder blade and lateral to the spine. 2% AraC was delivered for 10-14 days to ablate cycling cells in the SVZ.

Tamoxifen induction

For tamoxifen induction *in vivo*, at or after 6 weeks of age, animals were fed tamoxifen food (Harlan) for 2 weeks and then switched to a high fat diet during a chase period of 2-3 weeks. Tamoxifen food was custom formulated to contain 0.5% TAM and 5% sucrose by weight and blue dye (to enable monitoring of consumption based on color of feces) in a high fat base (Harlan Diet 2019). For tamoxifen induction *in vitro*, 1mM OH-Tamoxifen (H7904, Sigma) was added every other day, for 7 days.

Adeno Associated Virus (AAV) Viral injections

AAV5-GFAP(0.7)^{promoter}-mCherry-T2A-mAscl1-WPRE (AAV5-Gfap-*Ascl1*-T2A-*mCherry*; 3.9 x 10^{13} GC/mL) and AAV5-GFAP(0.7)^{promoter}-mCherry-WPRE (AAV5-Gfap-*mCherry*; 2.9 x 10^{13} GC/mL) particles were purchased from VectorBioLabs. 1uL of AAV was injected into the injured cortex of NestinCreER^{T2};YFP^{fl} mice 7d post stroke at a rate of 0.1mL/min at the following

coordinates: 0.6 AP, 2.25 ML, -1 DV, 1.6 AP, 2.25ML -1 DV and -1 AP, 2.25 ML, -1 DV, relative to bregma. The needle was left in place for 10 minutes after AAV injection to prevent backflow and then slowly withdrawn.

5-ethynyl-2´-deoxyuridine (EdU) injections

250 mg/kg EdU (Life Technologies, E10187) was injected intraperitoneally once daily for either 2 or 4 days after stroke.

Tissue processing, immunohistochemistry and quantification.

Mice were anesthetized with Avertin, perfused transcardially and postfixed for 2 hours with 4% paraformaldehyde. Brains were cryopreserved in 30% sucrose, frozen and 18 μm coronal cryostat sections were cut.

Cryosections were blocked with 10% normal goat serum (NGS) and 0.3% triton in PBS and labeled with a primary antibody in PBS overnight at 4C, followed by incubation with a secondary antibody and a nuclear stain in PBS for 1h at room temperature (RT). For double and triple immunohistochemistry, sections were reblocked in 10% NGS and 0.3% triton in PBS, incubated with a primary antibody 4°C O/N and then with a secondary antibody at RT for 1h. Samples labeled with gt anti dcx primary antibody were blocked in 10% normal donkey serum and 0.3% triton in PBS and incubated O/N at RT. Samples labeled with anti Ch Alexa 488 secondary antibody were incubated for 2h at RT. For EdU

staining, a ClickiiT EdU imaging kit (Life Tech, C10337 and C103040) was used according to the manufacturer's instructions.

In vivo, overlapping expression of tdTOMATO and GFP or YFP and GFAP in cell bodies was quantified in three 40x confocal stacks in 3 coronal sections per animal. For quantification of EdU or dcx and YFP, three 20x confocal stacks in 3 coronal sections per animal were obtained. For analysis of mCherry, YFP and neuronal markers, at least 100 cells were counted in at least three 20x confocal stacks per animal. Imaging was performed using Zen 2011 software and a Zeiss two-photon microscope, Velocity software and a Zeiss spinning disc confocal or Axiovision software and a Zeiss Observer Z1 inverted fluorescence microscope. Linear adjustments of contrast and brightness were made to micrographs using the respective microscope software. Threshold intensity was set according to the background signal detected in controls.

Summary of reagents used for immunohistochemistry

Primary Antibodies	**Dilution**	**Company**	**Catalogue Number**
Ms anti-β-III-tubulin (TUJ1)	1:500	Covance	MMS-435P-250
Rb anti-β-III-tubulin (TUJ1)	1:500	Covance	MRB-435P-100
Rb anti-GFAP	1:3000	DAKO	2016-04
Rb anti-S100β	1:200	DAKO	Z0311

Ms anti MAP2(a+b)	1:200	Sigma	M1406
Ms (IgM) anti O4	1:1000	R&D Systems	MAB1326
Rb anti KI-67	1:200	AbCam	Ab15580
Ch anti GFP	1:1000	Aves	GFP-1020
Rb anti RFP	1:2000	Rockland	600-401-379
Rb anti NeuN	1:100	Millipore	ABN78
Gt anti DCX	1:200	Santa Cruz	sc-8066
Secondary Antibodies	**Dilution**	**Company**	**Catalogue Number**
Anti ms IgM Alexa 568	1:400	Life Tech	A21043
Anti-ms IgG Alexa 568	1:400	Life Tech	A11031
Anti-ms IgG Alexa 488	1:400	Life Tech	A11001
Anti ms IgG Alexa 647	1:400	Life Tech	A21236
Anti gt IgG Alexa 647	1:400	Life Tech	A21447
Anti rb Alexa 568	1:400	Life Tech	A11036
Anti rb Alexa 647	1:400	Life Tech	A21245
Anti ch Alexa 488	1:400	Life Tech	A11039

Nuclear Stains	Dilution	Company	Catalogue Number
DAPI	50ng/mL	Life Tech	D3571
TOPRO	1:1000	Life Tech	T3605

Neurosphere Culture

Adult mice were anesthetized with isoflurane and cervically dislocated. Animals were decapitated and the meninges were removed. For cortical dissections, coronal slices were made using a scalpel blade and the cortex was collected, taking care to avoid the corpus callosum. The SVZ was dissected as previously described (Coles-Takabe et al., 2008; Tropepe et al., 1997). The tissue was enzymatically and mechanically dissociated into a single-cell suspension. Cells were plated at clonal density (5 cells/μL) in NS media (Neurobasal (Life Tech) containing L-glutamine (2 mM, Life Tech), penicillin/streptavidin (100 U/0.1 mg/ml (1x), Life Tech), B27 (1:50, Life Tech), epidermal growth factor (EGF; Sigma; 20ng/ml), fibroblast growth factor (FGF; Sigma; 10ng/ml), and heparin (2000ng/ml). For gangciclovir (GCV) ablation experiments, 20 μM GCV was added to the media before plating. After 10 days *in vitro*, the numbers of primary NSs was counted and the size of individual NSs was measured using Image J software (NIH). Primary NSs were grown for 10 days. For single sphere passaging, individual NSs were passaged every 7 days. For bulk sphere passaging, NSs were passaged every 7 days. NSs were

mechanically dissociated into a single-cell suspension, and replated under the same conditions as primary cultures. The number of ctxNSs per mouse was calculated as follows:

Number of cortical neurosphere forming cells per brain at 4d post stroke =

(number of cells after dissociation x number of neurospheres per well) / number of cells per well

Neurosphere differentiation immunocytochemistry and quantification.

One primary NS was plated per well of a 48-well plate coated with laminin (5 *µ*g/ml, Sigma) in differentiation medium (Neurobasal, Life Tech) containing L-glutamine (2 mM, Life Tech), penicillin/streptavidin (100 U/0.1 mg/ml (1x), Life Tech), B27 (1:50, Life Tech) and 1% fetal bovine serum (Life Tech). After 7 days of differentiation, cells were fixed with 4% paraformaldehyde.

For immunocytochemistry for cell phenotype markers, cell cultures were fixed in 4% PFA, blocked with 10% NGS in PBS and labeled with mouse anti-O4 overnight (O/N) at 4°C followed by an incubation with a secondary antibody. For double and triple immmunolabeling, cultures were re-blocked in 10% NGS and 0.3% triton in PBS and incubated with rabbit anti-GFAP and mouse anti-β-III-tubulin followed by incubation with a secondary antibody and DAPI. The number of phenotype marker positive cells and DAPI positive cells were quantified in three 10x photos per well. Images were captured using Zen 2011 software and a

Zeiss two-photon microscope or a Zeiss inverted microscope.

Reactive astrocyte culture

GFAP-CreER^{T2};YFP^{fl} adult mice were anesthetized with isoflurane and cervically dislocated at 4d post stroke. The meninges were removed and coronal slices were made using a scalpel blade. The cortex was collected, taking care to avoid the corpus callosum. The tissue was enzymatically and mechanically dissociated into a single-cell suspension. One cortical hemisphere was resuspended in 1mL of astrocyte media (DMEM/F12 (Life Tech) containing L-glutamine (2 mM, Life Tech), penicillin/streptavidin (100 U/0.1 mg/ml (1x), Life Tech), B27 (1:50, Life Tech), 0.45% glucose (Sigma, G8769) and 10% fetal bovine serum (FBS, Life Tech)) and plated in 2 wells of a 24 well poly-d-lysine coated plate. Media was changed the next day. Cultures could only be established from the ispsilateral hemisphere and never from the hemisphere contralateral to the stroke site.

Astrocyte conversion in vitro

Two days after reactive astrocyte culture establishment from GFAP-CreER^{T2};YFP^{fl} mice, 4-Hydroxytamoxifen (4-OH-TAM) was added to astrocyte media. Media + 4-OH-TAM was changed every other day for 5d. After 7d, cells were transfected with PBase, PB-CAG-rtTA (Woltjen et al., 2009) and PB- tetO-*Ascl1*-T2A-*Bfp* or CAG-*Ascl1*-IRES-*Dsred* using HD Fugene (Roche) at a ratio of

2:1. For control experiments either PB-tet-O-*B*fp or CAG-*Dsred* was used. The media was changed to N2B27 (50% Neurobasal (Life Tech) and 50% DMEM/F12 (Life Tech) containing B27 (1:50, Life Tech) and N2 (1:100, Life Tech). For PB-tetO-*Ascl1*-T2A-*Bfp* expression, 1500 ng/mL dox was added to the media. Media was changed every other day for the duration of the experiment.

The number of neurons was quantified by assessing converted neurons (TUJ1+YFP+BFP+ or TUJ1+YFP+dsred+ cells)/transfected astrocytes (YFP+BFP+ or YFP+DSRED+ cells).

Plasmids

PB-tetO-*Ascl1*-T2A-*Bfp*

Fusion PCR was used to amplify *Ascl1* and *Bfp* from Tet-O-FUW-*Ascl1* (Addgene) and pENTR-BFP and generate an attb PCR product with a T2A linker between *Ascl1* and *Bfp* and gateway overhangs using the following primers:

Attb_Ascl1_Fwd

5'GGGGACAAGTTTGTACAAAAAAGCAGGGTTCGCCACCATGGAGCAAAAGC TCATTT**3'**

Ascl1_T2A_Rev

5'CCTCTGCCCTCTCCGGATCCGAACCAGTTGGTAAAGTCC**3'**

T2A_BFP_Fwd

5'GGATCCGGAGAGGGCAGAGGAAGTCTGCTAACATGCGGTGACGTCGAGG AGAATCCTGGCCCCATGGTGAGCAAGGGCGAG**3'**

BFP_Attb_Rev

5'GGGGACCACTTTGTACAAGAAAGCTGGGTCTTACTTGTACAGCTGCTC**3'**

The attb PCR product was cloned using Gateway into pRetroX (Life Tech) and Piggybac transposon destination vectors. Vectors were sequenced for verification.

CAG-*Ascl1*-IRES-*Dsred* and CAG-*Dsred* were kind gifts from Magdalena Götz.

MACS and Image Stream FACS Analysis

Adult mice were anesthetized with isoflurane and cervically dislocated. Animals were decapitated at 4d post stroke. The meninges were removed and coronal slices were made using a scalpel blade. The cortex was collected, taking care to avoid the corpus callosum. The RMS was also dissected. The tissue was enzymatically and mechanically dissociated into a single-cell suspension. Cells were resuspended in MACS sorting buffer (Ca^{++} and Mg^{++} free PBS with 2% FBS and 1mM EDTA), stained with anti-PSA-NCAM-PE (1:100, Miltenyi Biotech, 30-093-274) and MACS sorted using a PE selection kit (Stem Cell Technologies, 18554) and an EasySep Magnet (Stem Cell Technologies, 18000), according to the manufacturer's instructions. For ImageStream analysis, dissociated cells were resuspended in 500uL of PBS (azide and serum/protein free) and stained with a fixable cell viability dye (FVD eFluor 780; eBioscience, 65-0865-14) according to the manufacturer's instructions. Cells were then washed with 10%

FBS in PBS, resuspended in 500 μL of MACS sorting buffer, stained with anti-PSA-NCAM-PE (1:100, Miltenyi Biotech, 30-093-274) or a mouse IgM-PE control (1:100, Miltenyi Biotech, 130-099-127), MACS sorted using a PE selection kit (Stem Cell Technologies, 18554) and an EasySep Magnet (Stem Cell Technologies, 18000), according to the manufacturer's instructions, stained with Hoescht (1 μg/mL, BD Biosciences, 33342) for 30 min at RT and resuspended in MACS sorting buffer. Cells from the MACS sorted fractions, column flow through (supernatant) fractions and unsorted cells from the injured cortex, uninjured (contralateral) cortex and RMS were analysed with an Amnis ImageStreamTM Mark II imaging flow cytometer (AMNIS). Single stained controls were collected for the compensation matrix. The resulting compensated image files were analysed using IDEAS analysis software (AMNIS). Focused, single cells were selected based on viability (exclusion of FVD e780 dye) and the presence of a nucleus (positive for Hoescht staining). The live nucleated cells were examined for PE-PSA-NCAM signal and the specific and punctate PSA-NCAM-PE binding to cells was described using the Bright Detail Intensity feature of the IDEAS software. The increased Bright Detail Intensity scores differentiated PSA-NCAM-PE binding from non-specific, diffuse binding of the IgM-PE isotype control. The antibody binding patterns were confirmed in composite cell images of bright field and PE fluorescence generated from the ImageStream data.

Analysis of the RMS supernatant showed high purity (only one cell escaped the column).

Data Acquisition and Statistical Analysis

All experiments were conducted blind, using a numbering system. F tests were used to compare variance between groups. Unpaired two-tailed *t* tests or unpaired two-tailed *t* tests with Welch's correction (for unequal variance) were used for comparisons between two groups. One-factor ANOVA was used followed by post hoc analysis (Tukey's or Dunnet's test) for comparisons between three or more groups. Comparison of percentages between groups was done using two sample z-tests for individual proportions. Differences were considered significant at $p < 0.05$. Values are presented as mean ± SEM.

Supplemental References

Tennant, K.A., and Jones, T.A. (2009). Sensorimotor behavioral effects of endothelin-1 induced small cortical infarcts in C57BL/6 mice. Journal of neuroscience methods *181*, 18-26.